A Survey on Ear Biometrics

AYMAN ABAZA, WVHTC Foundation
ARUN ROSS, West Virginia University
CHRISTINA HEBERT, and MARY ANN F. HARRISON, WVHTC Foundation
MARK S. NIXON, University of Southampton

Recognizing people by their ear has recently received significant attention in the literature. Several reasons account for this trend: first, ear recognition does not suffer from some problems associated with other non-contact biometrics, such as face recognition; second, it is the most promising candidate for combination with the face in the context of multi-pose face recognition; and third, the ear can be used for human recognition in surveillance videos where the face may be occluded completely or in part. Further, the ear appears to degrade little with age. Even though current ear detection and recognition systems have reached a certain level of maturity, their success is limited to controlled indoor conditions. In addition to variation in illumination, other open research problems include hair occlusion, earprint forensics, ear symmetry, ear classification, and ear individuality.

This article provides a detailed survey of research conducted in ear detection and recognition. It provides an up-to-date review of the existing literature revealing the current state-of-art for not only those who are working in this area but also for those who might exploit this new approach. Furthermore, it offers insights into some unsolved ear recognition problems as well as ear databases available for researchers.

1. INTRODUCTION

The science of establishing human identity based on the physical (e.g., fingerprints and iris) or behavioral (e.g., gait) attributes of an individual is referred to as biometrics [Jain et al. 2004]. Humans have used body characteristics such as face and voice for thousands of years to recognize each other. In contemporary society, there is a pronounced interest in developing machine recognition systems that can be used for

ACM Computing Surveys, Vol. 45, No. 2, Article 22, Publication date: February 2013.
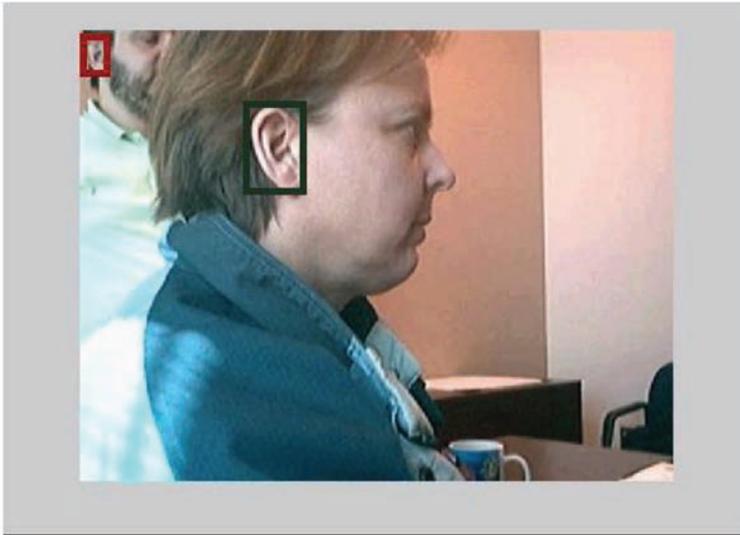
22

Fig. 1.   The ear biometric has tremendous potential when the side profile of a face image is available. In this example, the ear is much more easily observable than the frontal part of the face.

automated human recognition. With applications ranging from forensics to national security, biometrics is slowly becoming an integral part of modern society. The most common biometric systems are those based on characteristics that have been commonly used by humans for identification, such as fingerprint and face images, which have the largest market share. More recently, the iris biometric has been used in large-scale identity management systems such as border control applications. However, many other human characteristics are also being studied as possible biometric cues for human recognition. The ear structure is one such biometric cue, since the geometry and shape of the ear has been observed to have significant variation among individuals [Jain et al. 2004]. It is a prominent visible feature when the face is viewed in profile and, consequently, is readily collectable from video recording or photography. Figure 1 shows the side profile of some individuals where the ears are in a very clear pose compared to their frontal face.

In this article, we survey the current literature and outline the scientific work conducted in ear biometrics as well as clarify some of the terminology that has been introduced. There are existing surveys on ear biometrics including the ones by Lammi [2004], Pun and Moon [2004], and Islam et al. [2007]. Choras [2007] described feature extraction methods for ear biometric systems. Our goal for this survey is to expand on previous surveys by:

(1) including more than fifty ear publications from 2007–2010 that were not discussed in the previous surveys,
(2) adding references to available databases that are suitable for ear recognition studies,
(3) highlighting ear performance in multibiometric systems, and
(4) listing the open research problems in ear biometrics.

This article is organized as follows: Section 2 presents background information about ear anatomy, history of ear recognition in forensics, a brief description of a typical ear biometric system, and an overview of preliminary attempts that were made to create a working system; Section 3 presents most of the ear databases available for research;
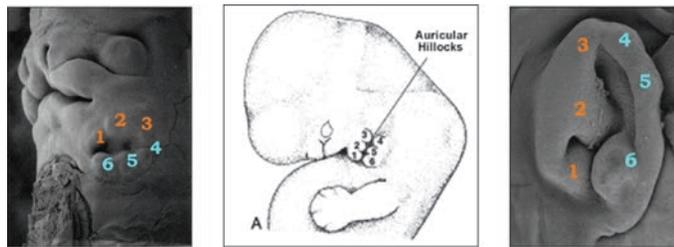
Fig. 2. The human ear develops from auricular hillocks (center) that arise in the 5th week of embryonic development. Between the 6th (left) and 9th (right) weeks of development, the hillocks enlarge, differentiate, and fuse to form the structures of the outer ear. Additionally, the ear translocates from the side of the neck to a more cranial and lateral site. This figure is taken from https://syllabus.med.unc.edu/courseware/ embryo_images/unit-ear/ear_htms/ear014.htm with permission of the School of Medicine, University of North Carolina.

Section 4 presents a survey of the various ear detection methods; the various feature extraction methods discussed in the literature are presented in Section 5; Section 6 discusses the role of the ear in multibiometric systems; and, finally, Section 7 highlights some of the open research areas in the field.

2. BACKGROUND

2.1. Ear Anatomy and Development

The ear starts to appear between the fifth and seventh weeks of pregnancy. At this stage, the embryo's face takes on more definition as a mouth perforation, nostrils, and ear indentations become visible. Though there is still disagreement as to the precise embryology of the external ear [ArbabZavar and Nixon 2011], the overall ear development during pregnancy is as follows.[1]

(1) The embryo develops initial clusters of embryonic cells that serve as the foundation from which a body part or organ develops. Two of these clusters, termed the first and second pharyngeal arches, form six tissue elevations called auricular hillocks during the fifth week of development. Figure 2 (center) shows a sketch of the embryo with the six auricular hillocks, labeled 1 through 6. Figure 2 (left) shows the growth and development of the hillocks after the sixth week of embryonic development.

(2) In the seventh week, the auricular hillocks begin to enlarge, differentiate, and fuse, producing the final shape of the ear, which is gradually translocated from the side of the neck to a more cranial and lateral site. By the ninth week, shown in Figure 2 (right), the morphology of the hillocks is recognizable as a human ear. Hillocks 1–3 form the first arch of the ear (tragus, helix, and cymba concha), while hillocks 4–6 form the second arch of the ear (antitragus, antihelix, and concha).

The external anatomy of the ear[2] is illustrated in Figure 3. The forensic science literature reports that ear growth after the first four months of birth is highly linear [Iannarelli 1989]. The rate of stretching is approximately five times greater than normal during the period from four months to the age of eight, after which it is constant until around the age of seventy when it again increases.

2.2. Ear Biometric Systems

An ear biometric system may be viewed as a typical pattern recognition system where the input image is reduced to a set of features that is subsequently used to compare

---

[1]https://syllabus.med.unc.edu/courseware/embryo_images/unit-ear/ear_htms/ear014.htm.
[2]http://www.plasticsurgery4u.com/procedure_folder/otoplasty_anatomy.html.

(1) Helix Rim
(2) Lobule
(3) Antihelix
(4) Concha
(5) Tragus
(6) Antitragus
(7) Crus of Helix
(8) Triangular Fossa
(9) Incisure Intertragica

Fig. 3.   External anatomy of the ear. The visible flap is often referred to as the *pinna*. The intricate structure of the pinna coupled with its morphology is believed to be unique to an individual although large-scale evaluation of automated ear recognition has not been conducted.
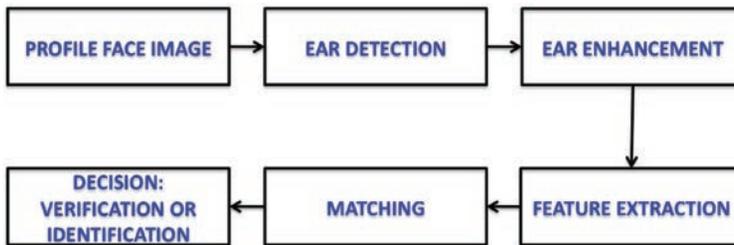
Fig. 4.   The block diagram of a typical ear recognition system.

against the feature sets of other images in order to determine its identity. Ear recognition can be accomplished using 2D images of the ear or 3D point clouds that capture the three-dimensional details of the ear surface. The ear biometric system has two possible modes of operation. In the *verification* mode, where the subject claims an identity, the input image is compared against that of the claimed identity via their respective feature sets in order to validate the claim. In the *identification* mode, where the subject does not claim an identity, the input ear image is compared against a set of labeled[3] ear images in a database in order to determine the best match and, therefore, its identity. The salient stages of a classical ear recognition system are illustrated in Figure 4.

(1) *Ear detection (segmentation).* The first and foremost stage involves localizing the position of the ear in an image. Here, a rectangular boundary is typically used to indicate the spatial extent of the ear in the given image. Ear detection is a critical component since the errors in this stage can undermine the utility of the biometric system.

(2) *Ear normalization and enhancement.* In this stage, the detected (segmented) ear is subjected to an enhancement routine that improves the fidelity of the image. Further, the ear image may be subjected to certain geometric or photometric corrections in order to facilitate feature extraction and matching. In some cases, a curve that tightly fits the external contour of the ear may be extracted.

(3) *Feature extraction.* While the segmented ear can be directly used during the matching stage, most systems extract a salient set of features to represent the ear. Feature extraction refers to the process in which the segmented ear is reduced to a mathematical model (e.g., a feature vector) that summarizes the discriminatory information.

---

[3]The term *labeled* is used to indicate that the identity of the images in the database is known.

Fig. 5.   Iannarelli's measurement.

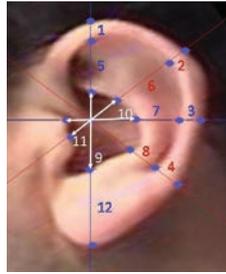(4) *Matching*. The features extracted in the previous stage have to be compared against those stored in the database in order to establish the identity of the input ear. In its simplest form, matching involves the generation of a match score by comparing the feature sets pertaining to two ear images. The match score indicates the similarity between two ear images.

(5) *Decision*. In the decision stage, the match score(s) generated in the matching module are used to render a final decision. In the verification mode of operation, the output is a "yes" or a "no", with the former indicating a genuine match and the latter indicating an impostor. In the identification mode of operation, the output is a list of potential matching identities sorted in terms of their match score.

2.3. Ear Recognition History

The potential of the human ear for personal identification was recognized and advocated as early as 1890 by the French criminologist Alphonse Bertillon [1896], who wrote[4]: "The ear, thanks to these multiple small valleys and hills which furrow across it, is the most significant factor from the point of view of identification. Immutable in its form since birth, resistant to the influences of environment and education, this organ remains, during the entire life, like the intangible legacy of heredity and of the intra-uterine life". Bertillon made use of the description and some measurements of the ear as part of the *Bertilllonage system* that was used to identify recidivists.

One of the first ear recognition systems is Iannarelli's system which was originally developed in 1949 [Iannarelli 1989]. This is a manual system based upon 12 measurements as illustrated in Figure 5. Each photograph of the ear is aligned such that the lower tip of a standardized vertical guide on the development easel touches the upper flesh line of the cocha area, while the upper tip touches the outline of the antitragus. Then the crus of helix is detected and used as a center point. Vertical, horizontal, diagonal, and anti-diagonal lines are drawn from that center point to intersect the internal and external curves on the surface of the pinna. The 12 measurements are derived from these intersections and used to represent the ear.

Fields et al. [1960] made an attempt to identify newborn babies in hospitals. They visually assessed 206 sets of ear photographs, and concluded that the morphological constancy of the ear can be used to establish the identity of the newborn.

Currently, there exists no commercial biometric system to automatically identify or verify the identity of individuals by way of their ear biometric. Burge and Burger [2000] presented one of the most cited ear biometric methods in the literature. They located the ear by using deformable contours on a Gaussian pyramid representation of the image gradient [Burge and Burger 1997]. Then they constructed a graph model from

----

[4]This statement is taken from Hurley et al. [2007].

the edges and curves within the ear, and invoked a graph-based matching algorithm for authentication. They do not report any performance measures on the proposed system.

Moreno et al. [1999] were the first to describe a fully automated system for ear recognition. They used multiple features and combined the results of several neural classifiers. Their feature vector included outer ear points, ear shape, and wrinkles, as well as macro-features extracted by a compression network. To test that system, two sets of images were acquired. The first set consisted of 168 images pertaining to 28 subjects with 6 photos per subject. The second set was composed of 20 images, corresponding to 20 different individuals. Later, Mu et al. [2004] extended this method. They represented the ear feature vector as a combination of the outer ear shape and inner ear structure. Then they employed a neural network for classification. This method can be considered as a simplified automation of Iannarelli's system [Iannarelli 1989].

Yuizono et al. [2002] treated the ear image recognition problem as regular search optimization problem, where they applied a Genetic Algorithm (GA) to minimize the mean square error between the probe and gallery images. They assembled a database of 660 images corresponding to 110 persons. They demonstrated an accuracy of 99-100%.

Like other biometric traits, research in ear recognition is directed by the databases that are available for algorithm evaluation and performance analysis. Therefore, we first discuss the various databases that have been assembled by multiple research groups for assessing the potential of ear biometrics.

3. DATABASES

Test and development of robust ear recognition algorithms require databases of sufficient size (many subjects, multiple samples per subject, etc.) that include carefully controlled variations of factors such as lighting and pose. In the literature, the Carreira-Perpinan [1995] database has been widely used; however, it is a very small database of 19 subjects. In this section, we review several databases that have been used in the literature of ear recognition (and detection). Most of these databases are either available for the public or can be transferred under license.

3.1. WVU Database

The West Virginia University (WVU) ear database was collected using the system [Fahmy et al. 2006] shown in Figure 6. This system had undergone various design, assembly, and implementation changes. The main hardware components for this system include the following.

—*PC*. It provides complete control of the moving parts and acquiring video from camera.
—*Camera*. It captures video. It is attached to the camera arm, and the latter is controlled by a stepper motor.
—*Linear Actuator*. This is a unique custom-made device (by Netmotion, Inc.) that has a 4-ft span and allows smooth, vertical (up or downward) translation. This device is used to adjust the height of the camera according to the subject height.
—*Light*. For this database, the light was fixed to the camera arm.
—*Structural Framework*. This consists of tinted wall, rotating arms, and other structural supports. A blackboard was added behind the chair to serve as a uniform background during video capture.

There are various software packages that were used: (i) Posteus IPE (stepper system control): to adjust the camera height, and to rotate the camera; (ii) EVI Series Demonstration Software (camera control): to adjust zoom, tilt, and focus of the used camera; and (iii) IC Video Capture: to record the subject's images during the camera rotation.

The WVU ear database consists of 460 video sequences for 402 different subjects, and multisequence for 54 subjects [Abaza 2008]. Each video begins at the left profile
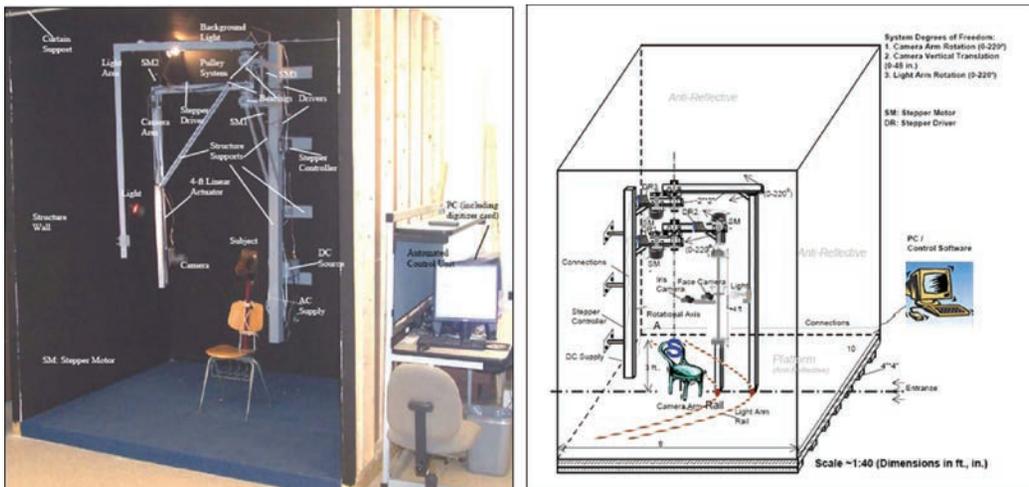
Fig. 6. The data acquisition system designed at West Virginia University for collecting ear images at multiple angles.

of a subject (0 degrees) and terminates at the right profile (180 degrees) in about 2 minutes. This database has 55 subjects with eyeglasses, 42 subjects with earrings, 38 subjects with partially occluded ears, and 2 fully occluded ears. The WVU database is currently not available for public use.

3.2. USTB Databases

The University of Science and Technology Beijing (USTB) databases[5] are available for academic research [USTB 2005].

—*IMAGE DATABASE I*. 180 images of 60 volunteers. For each subject the following three images were acquired: (a) normal ear image; (b) image with small angle rotation; and (c) image under a different lighting condition.
—*IMAGE DATABASE II*. 308 images of 77 volunteers. By defining the angle when the CCD camera is perpendicular to the ear as being the profile view ($0°$), for each subject the following four images were acquired: (a) profile image; (b) two images with $30°$ and $-30°$ angle variations; and (c) one with illumination variation.
—*IMAGE DATABASE III*. 79 volunteers. For each subject the following ear images were acquired:
  —*Regular ear images*. The subject rotates his head from 0 degrees to 60 degrees toward the right side. Images of the head were acquired at the following angles: $0°$, $5°$, $10°$, $15°$, $20°$, $25°$, $30°$, $40°$, $45°$, $50°$, $60°$. Two images were recorded at each angle resulting in a total of 22 images per subject. Similarly, as the subject rotates his head from 0 degrees to 45 degrees toward the left side, images of the head were acquired at the following angles: $0°$, $5°$, $10°$, $15°$, $20°$, $25°$, $30°$, $40°$, $45°$. Two images were recorded at each angle resulting in a total of 18 images per subject.
  —*Ear images with partial occlusion*. The total number of ear images with partial occlusion is 144 pertaining to 24 subjects with 6 images per subject. Occlusion is due to three conditions: partial occlusion (disturbance from some hair), trivial occlusion (little hair), and regular occlusion (natural occlusion due to hair).

---

[5] http://www1.ustb.edu.cn/resb/en/index.htm

Fig. 7. Image samples from USTB databases III [with permission of USTB].

Fig. 8. Image samples from UCR data set of color, (c) [Chen and Bhanu 2007] (IEEE reprinted with permission).

—*IMAGE DATABASE IV*. A camera system consisting of 17 CCD cameras, distributed around the subject at an interval of 15° between them, was used to acquire ear and face images of 500 volunteers at multiple poses/angles. Samples from USTB databases are shown in Figure 7.

3.3. UCR Database

The University of California Riverside (UCR) database was assembled from images captured by the Minolta Vivid 300 camera [Chen and Bhanu 2007]. This camera uses the light-stripe method to emit a horizontal stripe light to the object and the reflected light is then converted by triangulation into distance information. The camera outputs a range image and its registered color image in less than one second. The range image contains 200×200 grid points and each grid point has a 3D coordinate (x, y, z) and a set of color (r, g, b) values. The database contains 902 shots for 155 subjects. Each subject has at least four shots. There are 17 females; six subjects have earrings and 12 subjects have their ears partially occluded by hair (with less than 10% occlusion). The UCR database is currently not available to the public. Samples from USTB databases are shown in Figure 8.

3.4. UND Databases

The University of Notre Dame (UND) databases[6] are available to the public (free of charge). There are several collections for various modalities. The following are the collections that can be used for ear biometrics.

—*Collection E*. 464 visible-light face side profile (ear) images from 114 human subjects captured in 2002.

------

[6] http://www3.nd.edu/~cvrl/CVRL/Data_Sets.html.

Fig. 9.   Image samples from the UND databases [with permission of UND].
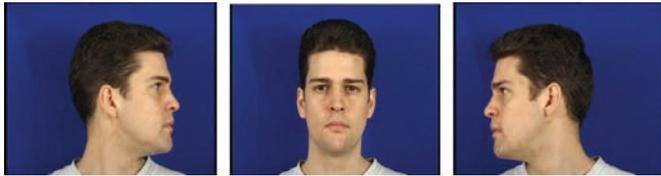
Fig. 10.   Image samples from XM2VTS face database (with permission of XM2VTS).

—*Collection F.* 942 3D (+ corresponding 2D) profile (ear) images from 302 human
   subjects captured in 2003 and 2004.
—*Collection G.* 738 3D (+ corresponding 2D) profile (ear) images from 235 human
   subjects captured between 2003 and 2005.
—*Collection J2.* 1800 3D (+ corresponding 2D) profile (ear) images from 415 human
   subjects captured between 2003 and 2005.

Figure 9 shows examples from the aforementioned collections of the UND databases.

3.5. XM2VTS Database

The XM2VTS database[7] was collected for research and development of identity veri-
fication systems using multimodal (face and voice) input data. The database contains
295 subjects, each recorded at four sessions over a period of 4 months. At each ses-
sion two head rotation shots (as shown in Figure 10) and six speech shots (subjects
reading three sentences twice) were recorded. Sets of data taken from this database
include high-quality color images, 32 KHz 16-bit sound files, video sequences, and a 3D
model [Messer et al. 1999]. The XM2VTS database is available for public use for a cost
[XM2VTSDB 1999].

3.6. UMIST Database

The UMIST Face database[8] contains 564 images of 20 subjects slowly rotating their
head from profile to frontal view. UMIST is a small database that is available to the
public, free of charge [Graham and Allison 1998; UMIST 1998]. In the literature, the
UMIST database was only used for ear detection experiments.

3.7. NIST Mugshot Identification Database (MID)

The NIST Mugshot Identification special database 18[9] contains both front and side
(profile) views when available (as shown in Figure 11). Separating front views and
profiles, there are 131 cases with two or more front views and 1418 with only one front

---

[7] http://www.ee.surrey.ac.uk/CVSSP/xm2vtsdb/.

[8] http://www.sheffield.ac.uk/eee/research/iel/research/face.

[9] http://www.nist.gov/srd/nistsd18.cfm.

Fig. 11.   Image samples from MID profile face database (with permission of NIST).

Fig. 12.   Image samples from FERET profile database (with permission of FERET).

view. Profiles have 89 cases with two or more profiles and 1268 with only one profile. Cases with both fronts and profiles have 89 cases with two or more of both fronts and profiles, 27 with two or more fronts and one profile, and 1217 with only one front and one profile. The MID database is available for public use for a cost [MID 1994]. In the literature, MID was used only for ear detection experiments.

3.8. FERET Database

The FERET[10] program set out to establish a large database of facial images that was gathered independently from the algorithm developers Phillips [1998] and Phillips et al. [2000]. The images were collected in a semi-controlled environment. To maintain a degree of consistency throughout the database, the same physical setup was used in each photography session. Because the equipment had to be reassembled for each session, there were some minor variations in images collected on different dates. The FERET database was collected in 15 sessions between August 1993 and July 1996. The database contains 1564 sets of images for a total of 14126 images that include 1199 individuals and 365 duplicate sets of images. For some individuals, images were collected at right and left profile (labeled pr and pl), as shown in Figure 12, and are suitable for 2D ear recognition. The FERET database is available for public use [FERET 2003].

3.9. CAS-PEAL Database

The CAS-PEAL[11] face database [Gao et al. 2004] is constructed by the Joint Research and Development Laboratory for Advanced Computer and Communication Technologies (JDL) of Chinese Academy of Sciences (CAS), under the support of the Chinese National Hi-Tech (863) Program and the ISVISION Tech. Co. Ltd. The CAS-PEAL database includes face images with various Poses, Expressions, Accessories, and Lighting (PEAL).

The CAS-PEAL face database contains 99,594 images of 1040 individuals (595 males and 445 females). For each subject, nine cameras spaced equally in a horizontal semi-

---

[10] http://www.itl.nist.gov/iad/humanid/feret/feret_master.html.

[11] http://www.jdl.ac.cn/peal/home.htm

Fig. 13.   Image samples from CAS-PEAL database (with permission of CASPEAL).

circular shelf are set up to simultaneously capture images across different poses in one shot (as shown in Figure 13). Each subject is also asked to look up and down to capture 18 images in another two shots. The CAS-PEAL database also includes 5 kinds of expressions, 6 kinds accessories (3 glasses, and 3 caps), and 15 lighting directions, as well as varying backgrounds, distance from cameras, and aging variation. The CAS-PEAL database is available for public use [Gao et al. 2008]. In the literature, the CAS-PEAL database was only used for ear detection experiments.

4. EAR DETECTION

Ear detection (segmentation) is an essential step for automated ear recognition systems, though many of the published recognition approaches achieve this manually. However, there have been several approaches aimed at providing fully automated ear detection. This section describes some of the semi-automated (computer-assisted) and automated techniques proposed in the literature. Table I summarizes these ear detection techniques.

4.1. Computer-Assisted Ear Segmentation

These semi-automated methods require user-defined landmarks specified on an image, and then ear segmentation is automated from that point onward. Yan and Bowyer [2005a] used a two-line landmark, with one line along the border between the ear and the face, and the other from the top of the ear to the bottom, in order to detect the ear region. Alvarez et al. [2005] proposed a modified snake algorithm and ovoid model technique. This technique requires the user to manually draw an approximated ear contour which is then used for estimating the ovoid model parameters for matching.

4.2. Template Matching Techniques

Burge and Burger [2000] located the ear using deformable contours on a Gaussian pyramid representation of the image gradient. Then edges are computed using the Canny operator, and edge relaxation is used to form larger curve segments, after which the remaining small curve segments are removed.

Ansari and Gupta [2007] used outer helix curves of ears moving parallel to each other as features for localizing the ear in an image. Using the Canny edge detector, edges are extracted from the whole image. These edges are segmented into convex and concave edges. From these segmented edges, expected outer helix edges are determined[12]. They assembled a database of 700 side faces, and reported an accuracy of $\sim 93\%$.

AbdelMottaleb and Zhou [2006] segmented the ear from a face profile based on template matching, where they modeled the ear by its external curve. Yuizono et al. [2002] also used a template matching technique for detection. They used both a hierarchical

---

[12]They observed that the ear resembles an ellipse in shape; hence they assumed that the shape of helix curve is convex.

Table I. Accuracy of Carious Ear Detection Techniques

Technique	Database Used	Accuracy
Template matching		
Burge and Burger[2000]	N/A	N/A
Ansari and Gupta[2007]	700 side faces	$\sim 93\%$
AbdelMottaleb and Zhou[2006]	103 subjects	N/A
Yuizono et al.[2002]	110 ($\times 3$) subjects	N/A
Chen and Bhanu[2004]	UCR, 30 subjects	$\sim 91.5\%$
Chen and Bhanu[2005b]	UCR,52 ($\times 6$) subjects	$\sim 92.6\%$
Shape based		
ArbabZavar and Nixon[2007]	XM2VTS, 252 images	100%
	UND, F	91%
Zhou et al.[2010]	UND, F-142 images	100%
Morphological Operators		
HajSaid et al.[2008]	WVU, 376 ($\times 10$) subjects	90%
Hybrid Techniques		
Skin color and template based		
Prakash et al.[2009]	150 side faces	94%
Jet space similarity		
Watabe et al.[2008]	XM2VTS, 181 ($\times 2$) subjects	N/A
Shape of low-level features		
Cummings et al.[2010]	XM2VTS, 252 images	99.6%
2D Skin color and		
3D template based		
Chen and Bhanu[2007]	UCR, 902 subjects	99.3%
	UND, 700 subjects	87.71
Ear contour extraction		
Yan and Bowyer[2007]		
	UND, 415 subjects (color)	79%
	UND, 415 subjects (depth)	85%
Haar-based		
Islam et al.[2008.b]	UND, 203 images	100%
	XM2VTS, 104 occluded	52%
Yuan and Zhang[2009]	CASPEAL, 166 images	FRR=3.0, FAR=3.6
	UMIST, 48 images	FRR=2.1, FAR=0
	USTB, 220 images	FRR=0.5, FAR=2.3
Abaza et al.[2010]	UMIST, 225 images	FRR=0, FAR=1.33
	UND, 940 images	FRR=5.63, FAR=5.85
	WVHTF, 228 images	FRR=6.14, FAR=1.32
	USTB, 720 images	FRR=6.25, FAR=1.81
	FERET, 100 occluded	FRR=35, FAR=3
Ear contour extraction		
Yan and Bowyer[2007]		
	UND, 415 subjects (color)	79%
	UND, 415 subjects (depth)	85%

pyramid and sequential similarity computation to speed up the detection of the ear from 2D images.

In the context of 3D ear detection, Chen and Bhanu [2004] used a model-based (template matching) technique for ear detection. The model template is represented by an averaged histogram of shape index[13]. The detection is a four-step process: step edge detection and thresholding, image dilation, connected component labeling, and template matching. Based on a test set of 30 subjects from the UCR database, they achieved a 91.5% detection rate with 2.52% false alarm rate. Later, Chen and Bhanu [2005b] developed another shape-model-based technique for locating human ears in side face range images where the ear shape model is represented by a set of discrete 3D ver-

---

[13]Shape index is a quantitative measure of the shape of a surface at each point, and is represented as a function of the maximum and minimum principal curvatures.

tices corresponding to the helix and anti-helix parts. They started by locating the edge segments and grouping them into different clusters that are potential ear candidates. For each cluster, they register the ear shape model with the edges. The region with the minimum mean registration error is declared to be the detected ear region. Based on 52 subjects from the UCR database, with 6 images per subject, they achieved a 92.6% detection rate.

4.3. Shape Based

ArbabZavar and Nixon [2007] enrolled the ear based on finding the elliptical shape of the ear using a Hough Transform (HT). They achieved a 100% detection rate using the XM2VTS face profile database consisting of 252 images from 63 subjects, and 91% using the UND, collection F, database.

In the context of 3D ear detection, Zhou et al. [2010] introduced a novel shape-based feature set, termed the Histograms of Categorized Shapes (HCS), for robust 3D ear detection. They used a sliding window approach and a linear Support Vector Machine (SVM) classifier. They reported a perfect detection rate, that is, a 100% detection rate with a 0% false positive rate, on a validation set consisting of 142 range profile images from the UND, collection F, database.

4.4. Morphological Operators Techniques

HajSaid et al. [2008] addressed the problem of a fully automated ear segmentation scheme by employing morphological operators. They used low computational cost appearance-based features for segmentation, and a learning-based Bayesian classifier for determining whether the output of the segmentation is incorrect or not. They achieved a 90% accuracy on 3750 facial images corresponding to 376 subjects in the WVU database.

4.5. Hybrid Techniques

Prakash et al. used skin color and template-based technique for automatic ear detection in a side profile face image [Prakash et al. 2009, 2008]. The technique first separates skin regions from nonskin regions and then searches for the ear within the skin regions using a template matching approach. Finally, the ear region is validated using a moment-based shape descriptor. Experimentation was done on an assembled database of 150 side profile face images, and yielded a 94% accuracy.

Watabe et al. [2008] introduced the notion of "jet space similarity" for ear detection, which denotes the similarity between Gabor jets and reconstructed jets obtained via Principal Component Analysis (PCA). They used the XM2VTS database for evaluation; however, they did not report their algorithm's accuracy.

Cummings et al. [2010] used the image ray transform, based upon an analogy to light rays, to detect ears in an image. This transformation is capable of highlighting tubular structures such as the helix of the ear and spectacle frames. By exploiting the elliptical shape of the helix, this method was used to segment the ear region. This technique achieved a detection rate of 99.6% using the XM2VTS database.

Chen and Bhanu [2007] fused skin color from color images and edges from range images to perform ear detection. In the range images, they observed that the edge magnitude is larger around the helix and the antihelix parts. They clustered the resulting edge segments and deleted the short irrelevant edges. Using the UCR database, they reported a correct detection rate of 99.3% (896 out of 902). Using the UND databases (collections F and a subset of G), they reported a correct detection rate of 87.71% (614 out of 700).

Yan and Bowyer developed a fully automatic ear contour extraction algorithm [Yan and Bowyer 2007, 2006]. First, they detected the ear pit based on the nose po-

sition and by searching within a sector. Then, they segmented the ear contour using the active contour initialized around the ear tip. In Yan and Bowyer [2007], using only color information, 88 out of 415 (21%) images were incorrectly segmented, while using only depth information, 60 out of 415 (15%) images were incorrectly segmented. They speculated that all of the incorrectly segmented images in these two situations could be correctly segmented by using a combination of color and depth information; however, experimental results corroborating this were not reported.

4.6. Haar Based

Islam et al. [2008b] used a cascaded Adaboost technique based on Haar features for ear detection. This technique is widely known in the domain of face detection as the Viola-Jones method [Viola and Jones 2004]. It is a very fast and relatively robust face detection technique. They trained the Adaboost classifier to detect the ear region, even in the presence of occlusions and degradation in image quality (e.g., due to motion blur). They reported a 100% detection performance on the cascaded detector tested against 203 profile images from the UND database, with a false detection rate of $5x10^{-6}$. In a second experiment, they were able to detect 54 ears out of 104 partially occluded images from the XM2VTS database.

Yuan and Zhang [2009] used the same technique as Islam et al. They reported a very good detection rate even when there were multiple subjects in the same image. They used three test sets to compose a database of 434 images:

—166 images from the CAS-PEAL database with a False Rejection Rate (FRR) of 3.0% and a False Acceptance Rate (FAR) of 3.6%;
—48 images from the UMIST database with a FRR of 2.1% and no false acceptance;
—220 images from the USTB database with a FRR of 0.5% and FAR of 2.3%.

The main drawback of the original Viola-Jones technique is the training time, which can take several weeks in some cases. Wu et al. [2008] modified the original approach for face detection to reduce the complexity of the training phase of the naive Adaboost by two orders of magnitude. Abaza et al. [2010] applied the modified Viola-Jones technique for ear detection. The training phase of their approach is about 80 times faster than the original Viola-Jones method, and achieves $\sim 95\%$ accuracy on four different test sets (> 2000 profile images for ~ 450 persons). They presented experiments showing robust detection in the presence of partial occlusion, noise, and multiple ears at various resolutions.

5. EAR RECOGNITION SYSTEMS

In this section, we examine the various ear recognition algorithms proposed in the literature and attempt to categorize them based on the feature extraction scheme used to represent the ear biometric. Table II summarizes these ear recognition systems.

5.1. Intensity Based

Victor et al. [2002] and Chang et al. [2003] built a multimodal recognition system based on face and ear. For the ear images the manually identified coordinates of the triangular fossa and the antitragus are used for ear detection. Their ear recognition system was based on the concept of eigen-ears, using Principal Component Analysis (PCA). They reported a performance of 72.7% for the ear in one experiment, compared to 90.9% for the multimodal system, using 114 subjects from the UND, collection E, database.

Zhang et al. [2005] built a hybrid system for ear recognition. This system combines Independent Component Analysis (ICA) and a Radial Basis Function (RBF) network. The original ear image database was decomposed into linear combinations of several

Table II. Various Ear Recognition Techniques

Technique	Database	Accuracy
Intensity-Based		
PCA, Chang et al.[2003]	UND, 114 sub	72.7%
ICA, Zhang et al.[2005]	Carreira Perpinan, 17 ($\times$6)	
	and 60 ($\times$3) sub	94.11%
FSLDA, Yuan and Mu[2007]	USTB, 79 ($\times$7) sub	90%
IDLLE, Xie and Mu[2008]	USTB, 79 sub [$-10°$ to $20°$]	$> 80\%$
	and [$0°$ to $10°$]	$> 90\%$
NKDA, Zhang and Liu[2008]	USTB, 60 sub	$R1 = 97.7\%$
Sparse Representation,	UND, 32 ($\times$6) sub	96.88%
Naseem et al.[2008]	USTB, 56 ($\times$5) sub	98.21%
Force Field (FF)		
Hurley et al.[2005a]	XM2VTS, 63 ($\times$4) sub	99.2%
FF then Contour extraction	29 ($\times$2) sub	
AbdelMottaleb and Zhou[2006]	against 103 sub	$R1 = 87.93\%$
FF then NKDFA	USTB, pose $25°$	75.3%
Dong and Mu[2008]	pose $30°$,	72.2%
	and pose $45°$	48.1%
2D Curves Geometry		
Choras and Choras[2006]	102 images	FRR=0-9.6%
Fourier Descriptor		
Abate et al.[2006]	70 sub [$0°$, $15°$, $30°$]	R1=[96%, 88%, 88%]
Wavelet Transformation		
Sana and Gupta[2007]	600 and 350 ($\times$3) sub	$> 96\%$
HaiLong and Mu[2009]	USTB II, 77 sub	85.7%
	USTB III, 79 sub	97.2%
Nosrati et al.[2007]	USTB	90.5%
	Carreira Perpinan, 17 ($\times$6) sub	95.05%
Wang et al.[2008]	USTB, [$5°$, $20°$],	[100%, 92.41%]
	and [$35°$, $45°$]	[62.66%, 42.41%]
Gabor Filters		
Yaqubi et al.[2008]	USTB, 60 ($\times$3) sub	75%
Nanni and Lumini[2009a]	UND, 114 sub	R1=84%
Gabor jets (EBGM)		
Watabe et al.[2008]	XM2VTS, 181 ($\times$2) sub	R1=98%
Log-Gabor Wavelets		
Kumar and Zhang[2007]	UND, 113 sub	90%
SIFT		
Kisku et al. [2009.a]	400 ($\times$2) sub	96.93%
Dewi and Yahagi[2006]	Carreira Perpinan, 17($\times$6) sub	78.8%
3D Features		
Yan et al.[2005]	UND, 302 sub	98.8%
Yan and Bowyer[2007]	UND, 415 sub	97.8%
Yan and Bowyer[2006]	UND, sub wearing ear rings	94.2%
3D local surface patch and ICP		
Chen and Bhanu[2005a]	UCR, 30 sub	93.3%
Chen and Bhanu[2007]	UCR, 155 and UND, 302 sub	96.8% and 96.4%
Single step ICP,		
Islam et al.[2008.a]	UND, 300 sub	R1=93.98%
AEM, Passalis et al.[2007]	UND, 415 ($\times$2) sub, 201	94.4%
	3D polygonals from 110 sub	plus Time Cut
2.5D, SFS	WVU, 402 galleries	R1=95.0%
Cadavid and AbdelMottaleb[2008b]	and 60 probes	EER=3.3%

sub: different subjects, EER: Equal Error Rate, FRR: False Reject Rate and R1: Rank one identification rate; otherwise the accuracy is the recognition rate

basic images. Then the corresponding coefficients of these combinations were fed into an RBF network. They achieved 94.11% using two databases of segmented ear images. The first database was the Carreira-Perpinan database [Carreira-Perpinan 1995] consisting of 102 grey-scale images (6 ear images for each of 17 subjects). The second

database was the USTB database I, consisting of 180 images (3 ear images for each of 60 subjects).

Yuan and Mu [2007] used an automatic ear extraction and normalization method based on an improved Active Shape Model (ASM). Ear normalization adjusts for any scaling and rotational variation of the ear image. Then Full-space Linear Discriminant Analysis (FSLDA) was applied to perform ear recognition. They used the USTB database III, consisting of 79 subjects and achieved a recognition rate of 90%, using a head rotation range varying between 20-degrees left-rotation to 10-degrees right-rotation.

Xie and Mu [2007] used an improved version of the locally linear embedding algorithm. Local Linear Embedding (LLE) is based on projecting data in high-dimensional space into a single global coordinate system of lower dimension, by preserving neighboring relationships, in order to discover the underlying structure of the data [Feng and Mu 2009]. LLE can better solve the problems of nonlinear dimensionality reduction; however, it suffers from lack of labeled information in the dataset. The improved version of LLE (IDLLE) first obtained the lower-dimensional representation of the data points using the standard LLE algorithm, and then adopted Linear Discriminant Analysis (LDA) to resolve the problem of human ear classification. They used 79 subjects from the USTB database IV, and they did not mention how they performed the detection and normalization steps. They reported the recognition rate of the multi-pose ear as 60.75% compared to 43.03% using regular LLE. Later they used the same database, with ear poses in the range $[-45°, 45°]$ [Xie and Mu 2008]. Experimentally they showed that the recognition rate of the multi-pose ear had improved using LLE, compared to PCA and Kernel PCA. They further showed that the improved version of the LLE algorithm is better, compared to the regular one at these poses. The recognition rate was above 80% for ear poses in the range $[-10°, 20°]$, and above 90% for those in the range $[0°, 10°]$.

Zhang and Liu [2008] examined the problem of multiview ear recognition. They used a B-spline pose manifold construction in a discriminative projection space. This space is formed by the Null Kernel Discriminant Analysis (NKDA) feature extraction scheme. They conducted many experiments and performed comparisons to demonstrate the effectiveness of their multiview ear recognition approach. Ears are segmented by manual supervising from original images and the segmented ear images are saved as a multiview ear dataset. They reported a 97.7% rank-1 recognition rate in the presence of large pose variations using 60 subjects from the USTB database IV.

Naseem et al. [2008] proposed a general classification algorithm for (image-based) object recognition, based on a sparse representation computed by $L1 - minimization$. This framework provides new insights into two crucial issues in ear recognition: feature extraction and robustness to occlusion [Wright et al. 2009]. From each image the ear portion is manually cropped, and no normalization of the ear region is needed. They conducted several experiments using the UND and the USTB databases with session variability, various head rotations, and different lighting conditions. These experiments yielded a high recognition rate in the order of 98%.

5.2. Force field

Hurley et al. used force field transformations for ear recognition [Hurley et al. 2000, 2005b]. The image is treated as an array of Gaussian attractors that act as the source of the force field (as shown in Figure 14). The directional properties of that force field are exploited to locate a small number of potential energy wells and channels that are used during the matching stage [Hurley et al. 2005a]. The fixed size frame was manually adjusted by eye to surround and crop the ear images. They reported a very
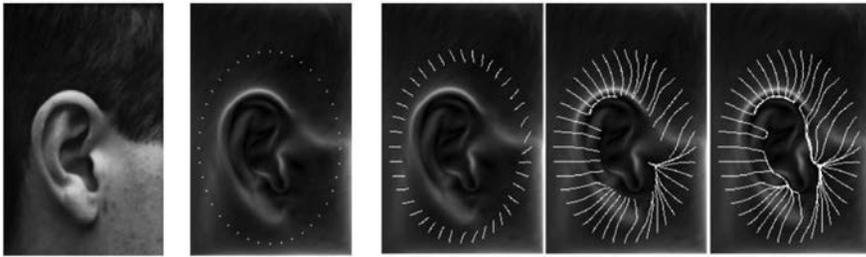
Fig. 14. Force field line formed by iterations [Hurley et al. 2000].

high recognition rate of 99.2%, using 4 images each of 63 subjects selected from the XM2VTS database.

AbdelMottaleb and Zhou [2006] used force field transformation followed by recognition based on contours constructed from these features. They assembled a database of profile face images from 103 subjects. For each person, one image was used for training, where the ear region was detected using external contour matching. The proposed ear recognition method was applied to 58 query images corresponding to 29 subjects. They achieved a 87.93% rank-1 recognition rate.

Dong and Mu used force field transformation and developed a two-stage approach for multi-pose ear feature extraction and recognition, that is, force field transformation plus null-space-based kernel fisher discriminant analysis (NKFDA) [Dong and Mu 2008]. The kernel technique can not only efficiently represent the nonlinear relation of data but also simplify the Null Linear Discriminant Analysis (NLDA). They cropped out the ear manually from the original images and made some preprocessing such as filtering and normalization. They used the USTB database IV and reported a recognition rate of 75.3% for pose $25°$, 72.2% for pose $30°$, 48.1% for pose $45°$.

5.3. 2D Ear Curves Geometry

Choras proposed an automated geometrical method [Choras 2004; 2005]. He extracted the ear contours and centroid from the ear image, and then constructed concentric circles using that centroid. He defined two feature vectors for the ear based on the interest points between the various contours of the ear and the concentric circles. Testing with an assembled database of 240 ear images (20 different views) for 12 subjects, and selecting images with very high quality and under ideal conditions of recognition, he reported a 100% recognition rate.

Later Choras and Choras [2006] added two more geometric feature vectors extracted using the angle-based contour representation and the geometrical parameters method. Then they conducted a comparison study using an assembled database of 102 ear images, where the various geometrical methods yielded a false reject rate between $(0 − 9.6\%)$.

5.4. Fourier Descriptor

Abate et al. [2006] used rotation-invariant descriptors, namely GFD (Generic Fourier Descriptor), to extract meaningful features from ear images. This descriptor is quite robust to both ear rotations and illumination changes. They assembled their own databases to evaluate the proposed scheme. The first dataset A contains 210 ear images from 70 subjects, with 3 samples for each subject: (a) looking ahead ($0°$ rotation), (b) looking up ($15°$ rotation), and (c) looking up ($30°$ rotation). Images were acquired over two sessions. The second dataset B was also obtained over two sessions, and contains

72 ear images from 36 subjects with 2 photos per subject looking up with a free rotation angle. Experimentally, they showed a marginally better rank-1 recognition rate (96%) compared to the eigen-ears algorithm (95%). Further, they showed that their technique had a rank-1 recognition rate of 88% for images obtained at 15° and 30° compared to a rate of 50% and 20% for the eigen-ears algorithm.

5.5. Wavelet Transformation

Sana and Gupta [2007] used a discrete Haar wavelet transform to extract the textural features of the ear. The ear was first detected from a raw image using a template matching technique. A Haar wavelet transform was then used to decompose the detected image and to compute coefficient matrices of the wavelet transforms which are clustered in its feature template. The matching score was calculated using the Hamming distance. They reported a recognition accuracy of 96% based on two databases: 600 subjects (3 images per subject) from the IITK database and 350 subjects from the Saugor database.

HaiLong and Mu [2009] used the low-frequency subimages, obtained by utilizing a two-dimensional wavelet transform, and then extracted features by applying an orthogonal centroid algorithm. They used the USTB databases, and they did not mention the detection step. They reported an average performance rate of 85.7% on the USTB database II (77 subjects) divided into four groups, and 97.2% on the USTB database IV (79 subjects), divided into 11 groups.

Nosrati et al. [2007] applied a 2D wavelet to the geometrically normalized (aligned) ear image. They used template matching for ear extraction, then they found three independent features in three directions (horizontal, vertical, and diagonal). They combined these decomposed images to generate a single feature matrix using the weighted sum. This technique allows one to consider the changes in the ear images simultaneously along three basic directions. Finally they applied PCA to the feature matrix for dimensionality reduction and classification. They achieved a recognition accuracy of 90.5% and 95.05% on the USTB database and Carreira-Perpinan database, respectively.

Wang et al. [2008] used Haar wavelet transforms and Uniform Local Binary Patterns (ULBPs) to recognize ear images. First, ear images were manually segmented and decomposed by a Haar wavelet transform. Then ULBPs were combined simultaneously with block-based and multiresolution methods to describe the texture features of ear subimages transformed by the Haar wavelet. Finally, the texture features were classified into identities using the nearest-neighbor method. Using the USTB database IV (no mention of ear detection), they conducted several experiments combining ULBPs with the multiresolution and block-based methods. They achieved a recognition rate of 100%, 92.41%, 62.66%, and 42.41% for pose angles of 5°, 20°, 35°, and 45°, respectively.

Feng and Mu [2009] also combined Local Binary Pattern (LBP) and wavelet transform. They used nonuniform $LBP_{8,1}$ operator, and evaluated the performance of various similarity measures and two matchers (K nearest-neighbor and two-class Support Vector Machine). They used images from USTB database III (no mention of ear detection): 79 subjects with 10 images per subject at various poses (0°, 5°, 10°, 15°, 20°).

5.6. Gabor Filters

Yaqubi et al. [2008] used a feature extraction method based on a set of Gabor filters followed by a maximization operation over multiple scales and positions. This method is motivated by a quantitative model of the visual cortex. Then they used Support Vector Machine (SVM) for ear classification. They obtained a recognition rate of 75% on a subset of the USTB ear database where 180 ear images were manually extracted from 60 subjects.

Fig. 15. The SIFT key points matching.

Nanni and Lumini used a multimatcher system, where each matcher was trained using features extracted from a single subwindow of the entire 2D image [Nanni and Lumini 2007; 2009a]. The ear was segmented using two landmarks. The features were extracted by the convolution of each subwindow with a bank of Gabor filters. Then their dimensionality was reduced using Laplacian eigen maps. The best matchers, corresponding to the most discriminative subwindows, were selected by running Sequential Forward Floating Selection (SFFS). Experiments were carried out using 114 subjects from the UND database (collection E) and the sum rule was employed for fusing the selected subwindows at the score level. They achieved a rank-1 recognition rate of $\sim$ 84% and a rank-5 recognition rate of $\sim$ 93%; for verification experiments, the area under the ROC curve was $\sim$ 98.5% suggesting very good performance. Later Nanni and Lumini [2009b] improved the performance of their ear matcher using score normalization. In order to discriminate between the genuine article and impostors, they trained a quadratic discriminant classifier. Their proposed a normalization method that overcomes the main drawback of the Unconstrained Cohort Normalization (UCN), as it does not need a large number of background models. Experimentally, they showed that for the ear modality, their proposed normalization and UCN reduces the EER from $\sim$ 11.6% to $\sim$ 7.6%.

Watabe et al. [2008] extended the ideas from elastic graph matching and Principal Component Analysis (PCA). For ear representation, they used an "ear graph" whose vertices were labeled by the Gabor jets of body of the antihelix, superior anti-helix crus, and inferior anti-helix crus. They developed a new ear detection algorithm, based on the notion of "jet space similarity," which denotes the similarity between Gabor jets and reconstructs jets obtained using PCA. They used 362 images, 2 per person, from the XM2VTS database for performance evaluation. In a verification experiment, they reported a FRR of 4% and a FAR of 0.1%, which was approximately 5 times better than the PCA technique. Further, in an identification experiment, the rank-1 recognition rate for their method was 98% compared to 81% for the PCA technique.

Kumar and Zhang [2007] used Log-Gabor wavelets to extract the phase information, that is, ear codes, from the 1D gray-level signals. Thus each ear is represented by a unique ear code or phase template. Then they compared the Hamming distance between the query ear images and the database as a classifier. They reported about 90% recognition using 113 subjects from the UND, collection E, database (no mention of the detection step).

5.7. Scale-Invariant Feature Transform (SIFT)

Dewi and Yahagi [2006] used SIFT to generate approximately 16 key-points for each ear image. Using the Carreira-Perpinan database (segmented ear images) [Carreira-Perpinan 1995], they reported a recognition rate of 78.8%.

Kisku et al. [2009a] used SIFT feature descriptors for structural representation of ear images (as shown in Figure 15). They developed an ear skin color model using Gaussian Mixture Model (GMM) and clustered the ear color pattern using vector quantization. Finally, they applied K-L divergence to the GMM framework for recording the color
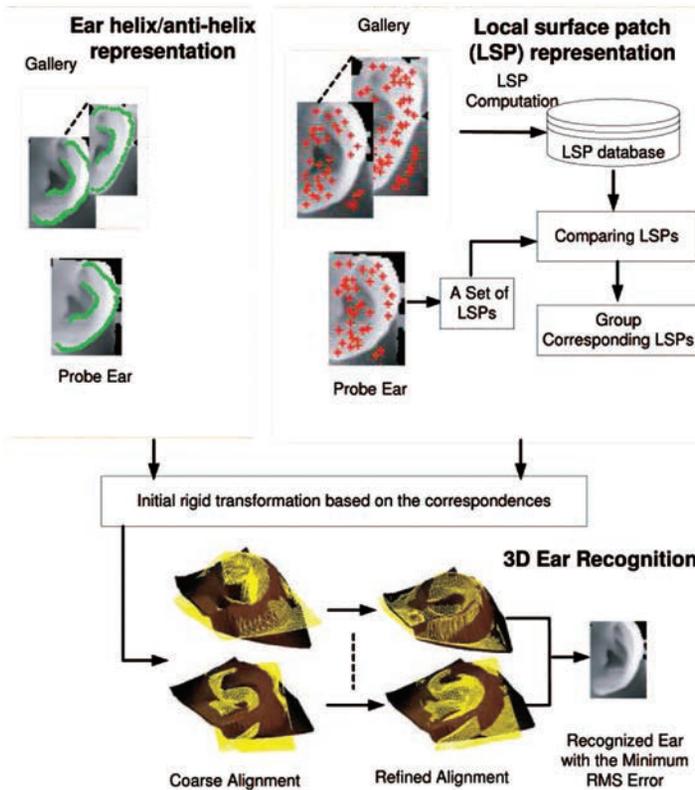
Fig. 16. The ear recognition module using the ear helix/antihelix and the Local Surface Patch (LSP) representations, (c) [Chen and Bhanu 2007]. IEEE, reprinted with permission.

similarity in the specified ranges by comparing color similarity between a pair of reference models and probe ear images. After manual segmentation of ear images in some color slice regions, they extracted SIFT key-points. They fused these features at feature level by augmenting a vector of extracted SIFT features. They tested using a locally collected ear database of 400 subjects with 2 images per subject, and the experimental results showed improvements in recognition accuracy by $\sim 3\%$.

5.8. 3D Ear

The only textbook describing ear biometrics [Bhanu and Chen 2008] focuses on a system for ear recognition using 3D shape. Chen and Bhanu [2005a] were the first to develop and experiment with a 3D ear biometric system. They used the shape-model-based technique for locating human ears in side face range images, and a Local Surface Patch (LSP) representation and the Iterative Closest Point (ICP) algorithm for ear recognition (as shown in Figure 16). In a small proof-of-concept experiment, they achieved a 93.3% recognition rate (2 errors out of 30), using manual segmentation. Chen and Bhanu [2007] conducted a larger experiment and automatic ear detection. They achieved a 96.77% rank-1 recognition rate (150 out of 155) using the UCR database and a 96.36% rank-1 recognition rate (291 out of 302) on the UND, collection F, database.

Yan et al. [2005] presented 3D ear recognition using ICP-based approaches. They used the UND, collection F, database, where they performed the segmentation step

using a two-line landmark. They reported rank-1 recognition rate as 98.8%. Only 4 images out of 302 were incorrectly matched due to poor data quality. Later Yan and Bowyer [2007] automated the ear detection by detecting the ear pit. They considered two approaches for matching points from the probe image to points on the gallery image using point-to-point and point-to-surface matching schemes. Their final algorithm attempted to exploit the trade-off between performance and speed. The point-to-point approach was used during the iterations to compute the transformation matrix relating the probe image with the gallery image. In an identification scenario, their algorithm achieved a rank-1 recognition rate of 97.8% using 415 subjects from the UND databases with 1,386 probes. They reported another experiment showing how the performance dropped with an increase in angle difference between the probe and gallery. In Yan and Bowyer [2006], they reported an experiment on a subset of users wearing earrings where the performance dropped to 94.2%.

Islam et al. [2008a] used ICP to implement a fully automated 3D ear recognition system. For the detection, first they used a 2D Haar-based ear detector, then they cropped the corresponding 3D segment. They used two subsets from the UND, collection F, database. The first subset consisted of arbitrarily selected 200 profile images of 100 different subjects, while the second database consisted of 300 subjects. They achieved a rank-1 recognition rate of 93% using single-step ICP.

Passalis et al. [2007] used a generic Annotated Ear Model (AEM) to register and fit each ear dataset. Only the 3D geometry that resides within a sphere of a certain radius that is centered roughly on the ear pit was automatically segmented. Then a compact biometric signature was extracted that retains 3D information. The meta-data containing this information were stored using a regular grid of lower dimension, allowing direct comparison. They used a database containing a 1031 dataset representing 525 subjects: 830 dataset representing 415 subjects from the UND database, and two hundred and one 3D polygonal dataset from 110 subjects. They achieved a recognition rate of 94.4% on this heterogeneous database. According to the literature, computing the similarity score for the 830 datasets from the UND database takes 276 hours on an average, while using their proposed method, it took approximately 7 hours for enrollment and a few minutes for authentication.

Cadavid and Abdel-Mottaleb described a novel approach for 3D ear biometrics from surveillance videos [Cadavid and AbdelMottaleb 2007; 2008a]. First they automatically segment the ear region using template matching and they reconstructed 2.5D images using the Shape from Shading (SFS) scheme. The resulting 2.5D models are then registered using the Iterative Closest Point (ICP) algorithm to calculate the similarity between the reference model and every model in the reference database. Later Cadavid and AbdelMottaleb [2008b] used the mathematical morphology ear detection technique [HajSaid et al. 2008], and they reported a 95.0% rank-1 recognition rate and 3.3% Equal Error Rate (EER) on the WVU database.

6. MULTIBIOMETRICS USING THE EAR MODALITY

In a multibiometric system, fusion can be accomplished at various levels [Ross et al. 2006]: fusion before matching (sensor and feature levels) and fusion after matching (match score, rank, and decision levels). Combining the ear biometric with the face modality has tremendous practical potential due to the following reasons: (a) the ear is part of the face; (b) the ear can be acquired using the same sensor as the face; and (c) the same type of feature extraction and matching algorithms can be used for both. Table III summarizes these multibiometric systems.

Table III. Ear in Multibiometric Systems

Multibiometrics	Fusion Level/ Method	Database	Accuracy
Face - ear			
Victor et al.[2002]			
Chang et al.[2003]	Image/ Data	UND, 114 sub	90.9%
Theoharis et al.[2008]	N/A	UND, F and G	R1=99.7%
Mahoor et al.[2009]	Score/ weighted SUM	WVU, 402 galleries	
		and 60 probes	100%
Islam et al.[2009]	Score/ weighted SUM	UND, F and G	R1=98.71%
Kisku et al. [2009.b]	Score/ Dempster Shafer	IITK, 400 ($\times$4) sub	95.53%
Face profile - ear			
Yuan et al.[2006.a]	Image/ Data	USTB	96.2%
Xu and Mu[2007b]	Score/ SUM and MED	USTB	97.62%
Pan et al.[2008],			
and Xu et al.[2007]	Feature/ weighted SUM	USTB	96.84%
Rahman and Ishikawa[2005]	Decision/ "manual"	UND, 18 sub	94.44%
Xu et al.[2007]	Feature/ weighted SUM	USTB, 38 sub	98.68%
Face - ear - 3 fingers			
Woodard et al.[2006]	Score/ MIN	UND, 85 sub	R1=97%
Face - ear - signature			
Monwar and Gavrilova[2009]	Rank/ Borda count	USTB, and	
	and Logistic regression	synthesized data	EER=1.12%
Ear - multiple algorithms			
Yan and Bowyer[2005b]	Score/ weighted SUM	UND, 302 sub	R1=98.7%
Zhang and Mu[2008]	Feature/ Concatenation	USTB, 79 sub	R1=55%
Srinivas and Gupta[2009]	Feature/ Merge	106($\times$10) sub	95.32%
ArbabZavar and Nixon[2011]	Score weighted SUM	XM2VTS, 150 sub	97.4%
Left and right ears			
Lu et al.[2006]	N/A	56 (5 left, 5 right) sub	R1=95.1%

sub: different subjects, EER: Equal Error rate, R1: Rank one identification rate; otherwise the accuracy is the recognition rate

6.1. Frontal Face and Ear

Victor et al. [2002] and Chang et al. [2003] discussed multimodal recognition systems using the ear and the face. They used the UND databases and reported a performance of 69.3% for face (PCA) and 72.7% for ear (PCA), in one experiment, compared to 90.9% for the multimodal system (PCA based on fused face and ear images). There have been other experiments based on eigen-faces and eigen-ears using different databases and other fusion rules.

(1) Darwish et al. [2009] fused the face and ear scores. They tested using 10 individuals (2 images each) from MIT, ORL (AT&T), and Yale databases, and reported an overall accuracy of 92.24%.

(2) Boodoo and Subramanian [2009] reported the same experiment using a database of 30 individuals (7 face and 7 ear images). They used 3 face and 3 ear images for testing. They considered two levels of fusion. The first method combined 3 images of the same modality using majority voting, while the second method fused the output of the two modalities using the AND rule. They reported a recognition rate of 96%.

(3) Luciano and Krzyzak [2009] presented a relatively wide experiment, where they used 100 subjects from the FERET database and 114 from the UND database. They reported good performance using face as a single modality, but not for the ear. Using normalized weighted scores, the best recognition rate of $\sim$ 99% was achieved using a weight in the range of (0.9 to 0.8)/(0.1 to 0.2) for face/ear respectively.

Middendorff and Bowyer [2007] and Middendorff et al. [2007] presented an overview of combining the frontal face and ear modalities, where they suggested several fusion methods for combining 2D and 3D data.

Theoharis et al. [2008] used a unified approach that fused 3D facial and ear data. An annotated deformable model was fitted to the data using ICP and Simulated Annealing (SA). Wavelet coefficients were computed from the geometry image and used as a biometric signature. The method was evaluated using the largest publicly available databases (FRGC v2 3D face database and the corresponding ears from the UND database, collections F and G). They reported a 99.7% rank-1 recognition rate but did not describe the fusion method.

Mahoor et al. [2009] used a multimodal 2.5D ear and 2D face biometric fused at score level. For 2.5D ear recognition, a series of frames was extracted from a video clip. The ear segment in each frame was independently reconstructed using the shape from shading method. Then various ear contours were extracted and registered using the iterative closest point algorithm. For 2D face recognition, a set of facial landmarks were extracted from frontal facial images using an active shape model. Then, the responses of facial images to a series of Gabor filters at the locations of facial landmarks were calculated, and used for recognition. They used the WVU database and reported a rank-1 identification rate of 81.67%, 95%, and 100% for face, ear, and fusion, respectively.

Islam et al. [2009] fused 3D local features for ear and face at score level, using the weighted sum rules. They used the FRGC v2 3D face database and the corresponding ears from the UND databases, collections F and G, and achieved a rank-1 identification rate of 98.71% and a verification rate of 99.68% (at 0.001 FAR) for neutral face expression. For other types of facial expressions, they achieved 98.1% and 96.83% identification and verification rates, respectively.

Kisku et al. [2009b] used Gabor filters to extract features of landmarked images of face and ear. They used a locally collected database of 1600 images from 400 subjects. Also they used a synthesized database where the face frontal images were taken from BANCA database [BaillyBailliere et al. 2003], and the ear images from the Carreira-Perpinan database [Carreira-Perpinan 1995]. They fused the scores using Dempster-Shafer (DS) decision theory, and reported an overall accuracy of 95.53%.

6.2. Face Profile and Ear

Yuan et al. [2006a] used face profile images that include the ear (assuming fusion at sensor / data level) and applied a full space linear discriminant analysis (i.e., using eigenvectors corresponding to positive eigenvalues). They used the USTB database and achieved a recognition rate of 96.2%.

Xu and Mu [2007b] used the same technique (full space linear discriminant analysis) for combining the face profile with the ear. They carried out decision fusion using the product, sum, and median rules according to Bayesian theory and a modified vote rule for two classifiers. They used the USTB database [USTB 2005] and achieved a recognition rate of 97.62% using the sum and median rules compared to 94.05% for the ear alone and 88.10% for the face profile alone.

References [Pan et al. 2008; Xu et al. 2007] presented a modified FDA technique by applying kernels of the feature vectors. They fused the face profile and ear at feature level (using average, product, and weighted-sum rules). They used the USTB database [USTB 2005] and achieved a recognition rate of 96.84% using the weighted-sum rule.

Xu and Mu [2007a] used Kernel Canonical Correlation Analysis (KCCA) for combining the face profile and the ear. They carried out decision fusion using the weighted-sum rule, where the weights are obtained by solving the corresponding Lagrangian. They used the 38 subjects from the USTB database and achieved a recognition rate of 98.68%.

Rahman and Ishikawa [2005] used the PCA technique to combine the face profile with the ear. They used a subset of 18 subjects (5 images each) from the UND database. They reported an identification rate of 94.44%.

6.3. Face, Ear, and Third Modality

Woodard et al. [2006] proposed combining 3D face images with ear and finger surfaces using score-level fusion. They reported a 97% rank-1 recognition rate based on a subset of 85 subjects from the UND 3D databases.

Monwar and Gavrilova [2008] developed a multimodal biometric system that used face, ear, and signature features extracted by PCA or Fisher's linear discriminant methods. The fusion is conducted at rank level. The ranks of individual matchers were combined using the Borda count method, the logistic regression method, or a modified Borda count method. To test this system, Monwar and Gavrilova used a chimeric database consisting of faces, ears, and signatures. For the face database, they used the Olivetti Research Lab (ORL) database [Samaria and Harter 1994], which contains 400 images, 10 each of 40 different subjects. For ear, they used the Carreira-Perpinan database [Carreira-Perpinan 1995]. For signatures, they used 160 signatures with 8 signatures of 20 individuals from the University of Rajshahi database [RUSign 2005]. Then those signatures were scanned. The results indicated that fusing individual modalities using weighted Borda count improved the overall Equal Error Rate (ERR) to 9.76% compared to an average of 16.78% for individual modalities. Later, Monwar and Gavrilova [2009] extended their experiment by including more data from the USTB database. For the signatures, also they used 500 signatures with 10 signatures of 50 individuals from Rajshahi database. They achieved an EER of 1.12 using the logistic regression rank fusion scheme.

6.4. Multi-Algorithmic Ear Recognition

Yan and Bowyer [2005b] used 2D PCA along with 3 different 3D ear recognition algorithms to combine the evidence due to 2D and 3D ear images. They used the UND databases, collection E, consisting of 1,884 (2D and 3D images) from 302 subjects. With the same database, using an improved ICP algorithm, they obtained a 98.7% rank-1 recognition rate by adopting a multi-instance approach on the 3D images.

Zhang and Mu [2008] extracted global features using the Kernel Principal Component Analysis (KPCA) technique and extracted local features using the Independent Component Analysis (ICA) technique. Then they established a correlation criterion function between two groups of feature vectors and extracted their canonical correlation features according to this criterion which could be viewed as fusion at feature level. They tested using the USTB database and achieved a rank-1 recognition rate of 55%, compared to 45% for the KPCA and 30% for the ICA alone.

Srinivas and Gupta [2009] used SIFT to extract the features from ear images at different poses and merged them according to a fusion rule in order to produce a single feature vector called the fused template. The similarity of SIFT features of the probe image and the enrolled user template was measured by their Euclidean distance. They collected 1060 images from 106 subjects. They captured 2 images at each of the following poses for the right ear: $[-40°, -20°, 0°, +20°, +40°]$. The images obtained were normalized to a size of 648×486. For training, they used three images per person for enrollment: images at poses $[-40°, 0° \ and + 40°]$. They tested using the remaining 7 images, and reported an accuracy of 95.32% for the fused template versus 88.33% for the nonfused template.

ArbabZavar and Nixon [2011] used a part-wise description model of the ear derived by a stochastic clustering on a set of scale-invariant features of a training set. They further enhanced the performance of this guided model description by incorporating a

wavelet-based ear recognition technique [ArbabZavar and Nixon 2008]. This wavelet-based analysis aims to capture information in the ear's boundary structures, which can augment discriminant variability. They presented several experiments using a weighted sum of the normalized distances based on the guided model and the wavelet-based technique. They tested these methods using 458 images of 150 subjects from the XM2VTS database. They achieved a recognition rate of $\sim 97.4\%$ compared to $\sim 89.1\%$ for the guided model and $\sim 91.9\%$ for the wavelet-based model.

6.5. Right Ear + Left Ear

Lu et al. [2006] extracted ear shape features using Active Shape Models (ASMs). They modeled the shape and local appearance of the ear in a statistical manner. In addition, steerable features were extracted from the ear image. Steerable features encode rich discriminant information of the local structural texture and provide guidance for shape location. The eigen-ear shape technique was used for final classification. Lu et al. [2006] conducted a small experiment to demonstrate how fusion of the results of the two ears can enhance the results[14]. They collected 10 images each from 56 individuals: 5 images for the left ear and 5 for the right ear, corresponding to 5 different poses. The difference in angle between two adjacent poses was 5 degrees. They achieved a rank-1 recognition rate of 95.1% via fusion versus 93.3% for the left ear or right ear alone.

7. OPEN RESEARCH AREAS

Research in ear biometrics is beginning to move out of its infant stage [Hurley et al. 2007]. While early research focused on ear recognition in constrained environments, the benefits of the ear biometric cannot be realized until the accompanying systems can work on large datasets in unconstrained surveillance-like environments. This means a number of research areas are relatively less explored with respect to this biometric.

7.1. Hair Occlusion

When the ear is partially occluded by hair or other artifacts, then methods for ear recognition can be severely impacted. Based on visual assessment of 200 occluded ear images from the FERET database, we determined that 81% of the hair occlusion is at the top of the ear, 17% from the side, and 2% at the bottom and other portions of the ear.

Burge and Burger [2000] suggested the use of thermogram images to detect occlusion due to hair and mask it out of the image. A thermogram image is one in which the surface heat of the subject is used to form an image. Figure 17 is a thermogram of the external ear. The subject's hair in this case has an ambient temperature between $27.2°C$ and $29.7°C$, while the external anatomy of the ear ranges from $30.0°C$ to $37.2°C$. Removing the hair is accomplished by segmenting out the low-temperature areas.

Yuan et al. [2006b] proposed an Improved Nonnegative Matrix Factorization with Sparseness Constraints (INMFSC) by imposing an additional constraint on the objective function of NMFSC. This improvement can control the sparseness of both the basis vectors and the coefficient matrix simultaneously. This proposed INMFSC was applied on normal images as well as partially occluded images. Experiments showed that their enhanced technique yielded better performance even with partially occluded images (as shown in Figure 18). Later Yuan et al. [2010] separated the normalized ear image into 28 subwindows as shown in Figure 19. Then, they used neighborhood-preserving embedding for feature extraction on each subwindow, and selected the most discriminative subwindows according to the recognition rate. Finally, they applied weighted

---

[14]Lu et al. [2006] did not provide details about the fusion level or method used.
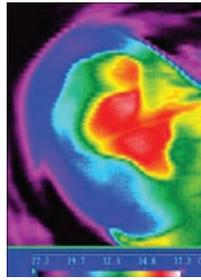
Fig. 17.   Ear thermogram, (c) [Burge and Burger 2000]. IEEE, reprinted with permission.
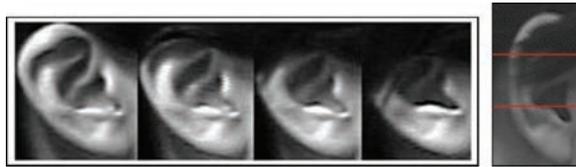

Fig. 18.   (a) Example of occluded ears; (b) splitting the ear image into three subregions; (c) [Yuan et al. 2006b]. IEEE, reprinted with permission.
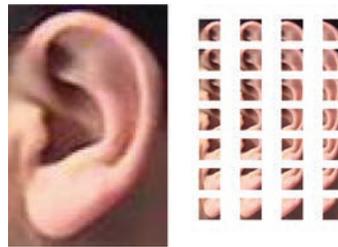

Fig. 19.   Ear image is divided into subwindows.

majority voting for fusion at decision level. They evaluated images of the ear that were partially occluded at the top, middle, bottom, left, and right of the ear, respectively, as shown in Figure 20.

Kocaman et al. [2009] applied Principal Component Analysis (PCA), Fisher Linear Discriminant Analysis (FLDA), Discriminative Common Vector Analysis (DCVA), and Locality-Preserving Projections (LPP) for ear recognition in the presence of occlusions. The error and hit rates of four algorithms were calculated by random subsampling and k-fold crossvalidation for various occlusion scenarios using a mask covering 15% of the test images.

ArbabZavar et al. [2007] used a Scale-Invariant Feature Transform (SIFT) to detect the features within the ear images. During recognition, given a profile image of the human head, the ear was enrolled and recognized from the various features selected by the model. They presented a comparison with PCA to show the advantage of the proposed model in handling occlusions. Later Bustard and Nixon [2008] evaluated the technique using various occlusion ratios and presented a rank-1 rate of 92% and 74% for 20% and 30%, respectively, for top-ear occlusion, and a rank-1 rate of 92% and 66% for 20% and 30%, respectively, for left-side occlusion.

In the context of constructing 3D models for the ear and face, one issue is that training data may contain noise and partial occlusion. Rather than exclude these regions manually, Bustard and Nixon developed a classifier which automates this process
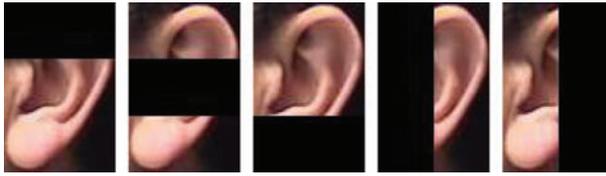
Fig. 20.   Test images using mask covering: (a) 33% top; (b) 33% middle; (c) 33% bottom; (d) 50% left; (e) 50% right.

Fig. 21.   Left ear; right ear; concatenated left and right ears; left ear and its mirror image.

[Bustard and Nixon 2010]. When combined with a robust registration algorithm the resulting system enabled full head morphable models to be constructed efficiently using less constrained data.

7.2. Ear Symmetry

Yan and Bowyer [2005a] conducted a small experiment to test ear symmetry using 119 subjects. The right ear of the subject was used as the gallery and the left ear was used as the probe. They concluded that most people's left and right ears are symmetric to a good extent, but that some people's left and right ears have different shapes.

Xiaoxun and Yunde [2007] conducted an experiment where the left and right ears were concatenated into a single image before mirror transformation (as shown in Figure 21). This concatenated image showed between 1-2% enhancement in performance compared to using the left or right ear alone.

Abaza and Ross [2010] presented a detailed analysis of the bilateral symmetry of human ears. They assessed the ear symmetry geometrically using symmetry operators and Iannarelli's measurements, where they studied the contribution of individual ear regions to the overall symmetry. Next, to assess the ear symmetry (or asymmetry) from a biometric recognition system perspective, they conducted several experiments using the WVU database. These experiments suggested the existence of some degree of symmetry in the human ears that can perhaps be systematically exploited in the future design of commercial ear recognition systems. Finally, they presented a case study, where they fused the scores of the right-right and the left ear image as gallery and the reflected right ear as probe (using weighted-sum rule). This fusion enhanced the overall performance by about 3%.

7.3. Earprint

Earprints, or earmarks, are marks left by secretions from the outer ears when someone presses up against a wall, door, or window. They are found in up to ∼ 15% of crime scenes [Rutty et al. 2005]. There have been several court cases in the U.S. and other countries where earprints have been used as physical evidence [Lynch 2000; Bamber 2001]; however, some convictions that relied on earprints have been overturned [Morgan 1999; Ede 2004]. The National Academy of Sciences report titled: "Strengthening Forensic Science in the United States: A Path Forward" provides an honest view of the limitations of forensic science, and presents a study on the admissibility of forensic evidence in litigation law and science.

Fig. 22. Examples of earprints in which various anatomical features are indicated. (1). helix; (2). crus of helix; (3-6). parts of antihelix; (7). tragus; (8). antitragus; (9). incisure intertragic; (10). lobe [Meijerman 2006].

It is commonly argued that earprints must be unique to an individual since the structure of the ear is unique to an individual. This line of reasoning has been disputed by others [Champod et al. 2001], on the basis that high variability in a three-dimensional malleable organ does not necessarily imply high variability in a two-dimensional mark produced by that organ. The parts of the ear which are most frequently found in earprints are the helix, anti-helix, tragus, and anti-tragus, while lesser-seen features include the earlobe, and the crus of helix (as shown in Figure 22) [Meijerman et al. 2004]. Specific details in these structures may contribute to the individualization of earprints. Such details include notches and angles in imprinted features, the positions of moles, folds, and wrinkles, and the position of pressure points [Meijerman et al. 2005]. However, individualization is confounded by several factors that cause substantial variation in earprints of the same ear.

—Variable deformations are caused by the force applied by the ear to the surface during listening [Meijerman et al. 2004, 2006a];
—There is duration of the ear's contact with the surface [Meijerman 2006];
—There are ornamental modifications to the ear, such as piercing [Meijerman 2006];
—Changes in the shape and size of the ear come due to aging [Meijerman et al. 2007].

Due to these factors, not even two prints of the same ear are exactly alike. In order for earprint recognition to be a viable biometric for forensics, intra-individual variation in earmarks must be distinguishable or significantly less than inter-individual variation. This is still an open and active area of research.

Though earprint recognition research is still at the initial stages, a few groups have developed methods for semiautomated or automated earprint recognition. Rutty et al. [2005] illustrated the concept of how to develop a computerized earprint identification system. First, they used a grid system using two anatomical landmarks to standardize the localization of the tags. Tags were allocated to each print at the sites of intersection of the grid lines with the anatomical structures. They did not involve performance data testing but rather they simplified the problem to whether or not the system and method employed could match the suspect print to that known within the database.

Meijerman et al. [2006b] proposed the first system for fully automated earmark recognition, and tested it with a small database of earprints taken from six sets of identical twins. Their method used key-point detection using the Difference of Gaussian (DoG) operator, after which they used the SIFT algorithm to transform each detected region into a 120-dimensional feature vector. Each key-point is then selected in turn and compared with all other key-points in the candidate print in order to look for matches, defining the best match as the one for which the Euclidean distance in the SIFT feature space is minimum. A geometric transformation is found that maximizes the number of matches. Finally, a similarity metric is defined as the number of key-point matches found between the pair of prints.

The Forensic Ear IDentification (FearID) project (funded by the 6th EU research framework) proposed to use weighted width, angular development, and anatomical annotation as distinctive features (semi-automatic system). Manual annotations on the prints and marks were performed before the matching process to facilitate the segmentation of the images and to locate anatomical points. With a set 7364 prints and 216 marks from 1229 donors, this approach resulted in Alberink and Ruifrok's [2007] EER of 3.9% for lab-quality prints and an EER of 9.3% for matching simulated marks against the prints database.

7.4. Ear Individuality

While the uniqueness (individuality) of the ear has been generally accepted to be true based on empirical results [Iannarelli 1989], the underlying scientific basis of ear individuality has not been formally established. As a result, the validity of ear (or earprint) evidence is now being challenged in several court cases.

In response to the U.S. appeals court ruling, a large-scale study involving 10,000 subjects has been proposed by Prof. Andre Moenssens to determine the variability of the ear across the population. In 1906, Imhofer studied a set of 500 ears and noted that he could clearly distinguish between each ear based on only 4 features [Hoogstrate et al. 2001]. Iannarelli [1989] also examined the difference in ear structures between fraternal and identical twins. He showed that even though their ear structures were similar, they were still clearly distinguishable. The results of these studies support the hypothesis that the ear has a unique physiological structure.

Burge and Burger [2000] presented a study of the ear individuality using Iannarelli's features [Iannarelli 1989]. Assuming an average standard deviation in the population of four units, the 12 Iannarelli's measurements provide a space with (4^{12}) variation which is less than 17 million distinct points. Purkait and Singh [2008] presented a preliminary study to test the individuality of human ear patterns. They manually extracted 12 inter-landmark linear distances from a set of 700 male and female individuals. They found that this 12-dimensional feature space could clearly distinguish more than 99.9% of ear pairs, where very few pairs had distances which fell below the safe distinction limit.

8. SUMMARY AND CONCLUSIONS

In this article, we have presented a survey of the ear biometric. We have considered two main stages of an ear recognition system: first is the detection stage and second is the features used for recognition. We have categorized the methods developed for these two steps, discussed their characteristics, and reported their performance. Even though current ear detection and recognition systems have reached a certain level of maturity, their success is limited to controlled indoor conditions. For example, to the best of our knowledge, ear biometrics have yet to be tested outdoors. In addition to variation in illumination, other open research problems include occlusion due to hair, ear symmetry, earprint forensics, ear classification, and ear individuality.

For any researcher who wants to start working on ear biometrics, we have presented a systematic discussion that includes available databases, detection and feature extraction techniques, as well as a survey of some unsolved ear recognition problems. The benefits of ear recognition are yet to be fully realized and we anticipate an extensive use of this biometric in next-generation face recognition systems.

REFERENCES

ABATE, A., NAPPI, M., RICCIO, D., AND RICCIARDI, S. 2006. Ear recognition by means of a rotation invariant descriptor. In *Proceedings of the 18ᵗʰ IEEE International Conference on Pattern Recognition (ICPR)*. 437–440.

ABAZA, A. 2008. High performance image processing techniques in automated identification systems. Ph.D. thesis, West Virginia University, Morgantown-WV.

ABAZA, A., HEBERT, C., AND HARRISON, M. F. 2010. Fast learning ear detection for real-time surveillance. In *Proceedings of the IEEE Conference on Biometrics: Theory, Applications, and Systems (BTAS)*.

ABAZA, A. AND ROSS, A. 2010. Towards understanding the symmetry of human ears: A biometric perspective. In *Proceedings of the IEEE Conference on Biometrics: Theory, Applications, and Systems (BTAS)*.

ABDELMOTTALEB, M. AND ZHOU, J. 2006. Human ear recognition from face profile images. In *Proceedings of the 2ⁿᵈ International Conference on Biometrics (ICB)*. 786–792.

ALBERINK, I. AND RUIFROK, A. 2007. Performance of the fearid earprint identification system. *Forensic Sci. Int. 166,* 145–154.

ALVAREZ, L., GONZALEZ, E., AND MAZORRA, L. 2005. Fitting ear contour using an ovoid model. In *Proceedings of the IEEE International Carnahan Conference on Security Technology*. 145–148.

ANSARI, S. AND GUPTA, P. 2007. Localization of ear using outer helix curve of the ear. In *Proceedings of the IEEE International Conference on Computing: Theory and Applications*. 688–692.

ARBAZZAVAR, B. AND NIXON, M. 2007. On shape-mediated enrolment in ear biometrics. In *Proceedings of the International Symposium on Visual Computing (ISVC)*. 549–558.

ARBAZZAVAR, B. AND NIXON, M. 2008. Robust log-gabor filter for ear biometrics. In *Proceedings of the 18ᵗʰ IEEE International Conference on Pattern Recognition (ICPR)*.

ARBAZZAVAR, B. AND NIXON, M. 2011. On guided model-based analysis for ear biometrics. *Comput. Vision Image Understand. 115,* 74, 487–502.

ARBAZZAVAR, B., NIXON, M., AND HURLEY, D. 2007. On model-based analysis of ear biometrics. In *Proceedings of the IEEE Conference on Biometrics: Theory, Applications, and Systems (BTAS)*.

BAILLYBAILLIERE, E., BENGIO, S., BIMBOT, F., HAMOUZ, M., KITTLER, J., MARIETHOZ, J., MATAS, J., MESSER, K., POPOVICI, V., POREE, F., RUIZ, B., AND THIRAN, J.-P. 2003. The banca database and evaluation protocol. In *Proceedings of the 4ᵗʰ International Conference on Audio- and Video-Based Biometric Person Authentication*. Vol. 2688. 625–638.

BAMBER, D. 2001. Prisoners to appeal as unique 'earprint' evidence is discredited. http://www.telegraph.co.uk/news/uknews/1364060/Prisoners-to-appeal-as-unique-earprint-evidence-is-discredited.html

BERTILLON, A. 1896. *Signaletic Instructions Including: The Theory and Practice of Anthropometrical Identification*. R.W. McClaughry translation, The Werner Company.

BHANU, B. AND CHEN, H. 2008. *Human Ear Recognition by Computer* 1ˢᵗ Ed. Springer.

BOODOO, N. B. AND SUBRAMANIAN, R. K. 2009. Robust multibiometric recognition using face and ear images. *Int. J. Comput. Sci. Inf. Secur. 6,* 2.

BURGE, M. AND BURGER, W. 1997. Ear biometrics for machine vision. In *Proceedings of the 21ˢᵗ Workshop of the Austrian Association for Pattern Recognition*.

BURGE, M. AND BURGER, W. 2000. Ear biometrics in computer vision. In *Proceedings of the 15ᵗʰ IEEE International Conference on Pattern Recognition (ICPR)*. 826–830.

BUSTARD, J. AND NIXON, M. 2008. Robust 2D ear registration and recognition based on SIFT point matching. In *Proceedings of the IEEE Conference on Biometrics: Theory, Applications, and Systems (BTAS)*.

BUSTARD, J. AND NIXON, M. 2010. 3D morphable model construction for robust ear and face recognition. In *Proceedings of the IEEE Conference on Computer Vision and Patern Recognition (CVPR)*.

CADAVID, S. AND ABDELMOTTALEB, M. 2007. Human identification based on 3D ear models. In *Proceedings of the 1ˢᵗ IEEE International Conference on Biometrics: Theory, Applications, and Systems (BTAS)*. 1–6.

CADAVID, S. AND ABDELMOTTALEB, M. 2008a. 3D ear modeling and recognition from video sequences using shape from shading. In *Proceedings of the 19ᵗʰ IEEE International Conference on Pattern Recognition (ICPR)*. 1–4.

CADAVID, S. AND ABDELMOTTALEB, M. 2008b. 3D ear modeling and recognition from video sequences using shape from shading. *IEEE Trans. Inf. Forens. Secur. 3*, 4, 709–718.

CARREIRA –PERPINAN, M. A. 1995. Compression neural networks for feature extraction: Application to human recognition from ear images. M.S. thesis, Faculty of Informatics, Technical University of Madrid, Spain.

CHAMPOD, C., EVETT, I., AND KUCHLER, B. 2001. Earmarks as evidence: A critical review. *Forens. Sci. 46,* 6, 1275–1284.

CHANG, K., BOWYER, K., SARKAR, S., AND VICTOR, B. 2003. Comparison and combination of ear and face images in appearance-based biometrics. *IEEE Trans. Pattern Anal. Mach. Intell. 25*, 1160–1165.

CHEN, H. AND BHANU, B. 2004. Human ear detection from side face range images. In *Proceedings of the IEEE International Conference on Pattern Recognition (ICPR)*. 574–577.

CHEN, H. AND BHANU, B. 2005a. Contour matching for 3D ear recognition. In *Proceedings of the IEEE Workshops on Application of Computer Vision (WACV)*. 123–128.

CHEN, H. AND BHANU, B. 2005b. Shape model-based 3D ear detection from side face range images. In *Proceedings of the IEEE Conference on Computer Vision and Pattern Recognition (CVPR)*. 122–127.

CHEN, H. AND BHANU, B. 2007. Human ear recognition in 3D. *IEEE Trans. Pattern Anal. Mach. Intell. 29,* 4, 718–737.

CHORAS, M. 2004. Human ear identification based on image analysis. In *Proceedings of the 7th IEEE International Conference on Artificial Intelligence and Soft Computing (ICAISC)*.

CHORAS, M. 2005. Ear biometrics based on geometrical feature extraction. *Electron. Lett. Comput. Vis. Image Anal. 5,* 3, 84–95.

CHORAS, M. 2007. Image feature extraction methods for ear biometrics – A survey. In *Proceedings of the 6th IEEE International Conference on Computer Information Systems and Industrial Management Applications*. 261–265.

CHORAS, M. AND CHORAS, R. 2006. Geometrical algorithms of ear contour shape representation and feature extraction. In *Proceedings of the 6th IEEE International Conference on Intelligent Systems Design and Applications (ISDA)*.

CUMMINGS, A., NIXON, M., AND CARTER, J. 2010. A novel ray analogy for enrollment of ear biometrics. In *Proceedings of the IEEE Conference on Biometrics: Theory, Applications, and Systems (BTAS)*.

DARWISH, A. A., ABDELGHAFAR, R., AND ALI, A. F. 2009. Multimodal face and ear images. *J. Comput. Sci. 5*, 5, 374–379.

DEWI, K. AND YAHAGI, T. 2006. Ear photo recognition using scale invariant keypoints. In *Proceedings of the International Computational Intelligence Conference*. 253–258.

DONG, J. AND MU, Z. 2008. Multi-Pose ear recognition based on force field transformation. In *Proceedings of the 2nd IEEE International Symposium on Intelligent Information Technology Application*. 771–775.

EDE, R. 2004. Wrongful convictions put forensic science in the dock. *The Times (London)*, February 3.

FAHMY, G., ELSHERBEENY, A., MANDALA, S., ABDELMOTTALEB, M., AND AMMAR, H. 2006. The effect of lighting direction/condition on the performance of face recognition algorithms. In *Proceedings of the SPIE Conference on Human Identification*.

FENG, J. AND MU, Z. 2009. Texture analysis for ear recognition using local feature descriptor and transform filter. *Proc. SPIE 7496*, 1.

FERET. 2003. Color FERET database. http ://face.nist.gov/colorf eret/

FIELDS, C., FALLS, H. C., WARREN, C. P., AND Z IMBEROFF, M. 1960. The ear of newborn as an identification constant. *Obstetr. Gynecol. 16*, 98–102.

GAO, W., CAO, B., SHAN, S., C HEN, X., Z HOU, D., ZHANG, X., AND ZHAO, D. 2008. CAS-PEAL the cas-peal large-scale chinese face database and baseline evaluations. *IEEE Trans. Syst. Man Cybernet. Part A Syst. Hum. 38,* 1, 149 – 161.

GAO, W., CAO, B., SHAN, S., Z HOU, D., ZHANG, X., AND ZHAO, D. 2004. CAS-PEAL. http ://www.jdl.ac.cn/peal/home.htm

GRAHAM, D. AND ALLISON, N. 1998. Characterizing virtual eigen-signatures for general-purpose face recognition. In *Face Recognition: From Theory to Applications*, Springer, 446–456.

HAILONG, Z. AND MU, Z. 2009. Combining wavelet transform and orthogonal centroid algorithm for ear recognition. In *Proceedings of the 2nd IEEE International Conference on Computer Science and Information Technology*.

HAJSAID, E., ABAZA, A., AND AMMAR, H. 2008. Ear segmentation in color facial images using mathematical morphology. In *Proceedings of the 6th IEEE Biometric Consortium Conference (BCC)*.

HOOGSTRATE, A., VANDEN HEUVEL, H., AND HUYBEN, E. 2001. Ear identification based on surveillance camera images. *Sci. Justice 41*, 3, 167–172.

HURLEY, D., ARBABZAVAR, B., AND NIXON, M. 2007. The ear as a bio-metric. In *Handbook of Biometrics*, Springer, 131–150.

HURLEY, D., NIXON, M., AND CARTER, J. 2000. Automatic ear recognition by force field transformations. In *Proceedings of the IEE Colloquium on Visual Biometrics*. 7/1–7/5.

HURLEY, D., NIXON, M., AND CARTER, J. 2005a. Ear biometrics by force field convergence. In *Proceedings of the 5th International Conference on Audio- and Video-Based Biometric Person Authentication (AVBPA)*. 386–394.

HURLEY, D., NIXON, M., AND CARTER, J. 2005b. Force field feature extraction for ear biometrics. *Comput. Vis. Image Understand. 98*, 3, 491–512.

IANNARELLI, A. 1989. *Ear Identification, Forensic Identification Series*. Paramount Publishing Company, Fremont, CA.

ISLAM, S., BENNAMOUN, M., AND DAVIES, R. 2008a. Fast and fully automatic ear detection using cascaded adaboost. In *Proceedings of the IEEE Workshop on Applications of Computer Vision*. 1–6.

ISLAM, S., BENNAMOUN, M., MIAN, A., AND DAVIES, R. 2008b. A fully automatic approach for human recognition from profile images using 2D and 3D ear data. In *Proceedings of the 4th International Symposium on 3D Data Processing Visualization and Transmission*.

ISLAM, S., BENNAMOUN, M., MIAN, A., AND DAVIES, R. 2009. Score level fusion of ear and face local 3D features for fast and expression-invariant human recognition. In *Proceedings of the 6th International Conference on Image Analysis and Recognition*. 387–396.

ISLAM, S., BENNAMOUN, M., OWENS, R., AND DAVIES, R. 2007. Biometric approaches of 2D-3D ear and face: A survey. In *Advances in Computer and Information Sciences and Engineering*, Springer, 509–514.

JAIN, A., ROSS, A., AND PRABHAKAR, S. 2004. An introduction to biometric recognition. *IEEE Trans. Circ. Syst. Video Technol. 14*, 1, 4–20.

KISKU, D. R., GUPTA, P., MEHROTRA, H., AND SING, J. K. 2009b. Multimodal belief fusion for face and ear biometrics. *Intell. Inf. Manag. 1*, 3.

KISKU, D. R., MEHROTRA, H., GUPTA, P., AND SING, J. K. 2009a. SIFT-Based ear recognition by fusion of detected key-points from color similarity slice regions. In *Proceedings of the IEEE International Conference on Advances in Computational Tools for Engineering Applications (ACTEA)*. 380–385.

KOCAMAN, B., KIRCI, M., GUNES, E. O., CAKIR, Y., AND OZBUDAK, O. 2009. On ear biometrics. In *Proceedings of the IEEE Region 8 Conference (EUROCON)*.

KUMAR, A. AND ZHANG, D. 2007. Ear authentication using log-gabor wavelets. In *SPIE Defence and Security Symposium*. Vol. 6539.

LAMMI, H. 2004. Ear biometrics. Tech. rep., Lappeenranta University of Technology.

LU, L., ZHANG, X., ZHAO, Y., AND JIA, Y. 2006. Ear recognition based on statistical shape model. In *Proceedings of the 1st IEEE International Conference on Innovative Computing, Information and Control*. 353–356.

LUCIANO, L. AND KRZYZAK, A. 2009. Automated multimodal biometrics using face and ear. In *Proceedings of the 6th International Conference on Image Analysis and Recognition (ICIAR)*. 451–460.

LYNCH, C. 2000. Ear-Prints provide evidence in court. *Glasgow University News*.

MAHOOR, M., CADAVID, S., AND ABDELMOTTALEB, M. 2009. Multimodal ear and face modeling and recognition. In *Proceedings of the IEEE International Conference on Image Processing (ICIP)*.

MEIJERMAN, L. 2006. Inter- and intra individual variation in earprints. Ph.D. thesis, University Leiden.

MEIJERMAN, L., NAGELKERKE, N., VAN BASTEN, R., VANDER LUGT, C., DECONTI, F., DRUSINI, A., GIACON, M., SHOLL, S., VANEZIS, P., AND MAAT, G. 2006a. Inter and Intra-individual variation in applied force when listening at a surface, and resulting variation in earprints. *Med. Sci. Law 46*, 141–151.

MEIJERMAN, L., SHOLL, S., DECONTI, F., GIACON, M., VANDER LUGT, C., DRUSINI, A., VANEZIS, P., AND MAAT, G. 2004. Exploratory study on classification and individualization of earprints. *Forens. Sci. Int. 140,* 91–99.

MEIJERMAN, L., THEAN, A., AND MAAT, G. 2005. Earprints in forensic investigations. *Forens. Sci. Med. Pathol. 1,* 4, 247–256.

MEIJERMAN, L., THEAN, A., VANDER LUGT, C., VAN MUNSTER, R., VANANTWERPEN, G., AND MAAT, G. 2006b. Individualization of earprints: Variation in prints of monozygotic twins. *Forens. Sci. Med. Pathol. 2,* 1, 39–49.

MEIJERMAN, L., VANDER LUGT, C., AND MAAT, G. 2007. Cross-Sectional anthropometric study of the external ear. *Forens. Sci. 52,* 286–293.

MESSER, K., MATAS, J., KITTLER, J., LUETTIN, J., AND MAITRE, G. 1999. XM2VTSDB: The extended M2VTS database. In *Proceedings of the 2nd International Conference on Audio and Video-Based Biometric Person Authentication*.

MID. 1994. NIST mugshot identification database. http://www.nist.gov/srd/nistsd18.cfm

MIDDENDORFF, C. AND BOWYER, K. 2007. Multibiometrics using face and ear. In *Handbook of Biometrics*, Springer, Chapter 16, 315–334.

MIDDENDORFF, C., BOWYER, K. W., AND YAN, P. 2007. Multimodal biometrics involving the human ear. In *Multimodal Surveillance: Sensors, Algorithms and Systems*, Artech House, Boston, Chapter 8, 177–190.

MONWAR, M. M. AND GAVRILOVA, M. 2008. FES: A system for combining face, ear and signature biometrics using rank level fusion. In *Proceedings of the 3rd IEEE International Conference on Information Technology: New Generations*. 922–927.

MONWAR, M. M. AND GAVRILOVA, M. 2009. Multimodal biometric system using rank-level fusion approach. *IEEE Trans. Syst. Man Cybern. B39*, 4.

MORENO, B., SANCHEZ, A., AND VELEZ, J. 1999. On the use of outer ear images for personal identification in security applications. In *Proceedings of the 33rd IEEE International Conference on Security Technology*. 469–476.

MORGAN, J. 1999. State v. Kunze, court of appeals of washington, division 2. 97 Wash.App. 832, 988 p.2d 977. http://www.forensic-evidence.com/site/ID/ID Kunze.html

MU, Z., YUAN, L., XU, Z., XI, D., AND QI, S. 2004. Shape and structural feature based ear recognition. In *Proceedings of the 5th Chinese Conference on Biometric Recognition*. 663–670.

NANNI, L. AND LUMINI, A. 2007. A multi-matcher for ear authentication. *Pattern Recogn. Lett. 28,* 16, 2219–2226.

NANNI, L. AND LUMINI, A. 2009a. Fusion of color spaces for ear authentication. *Pattern Recogn. 42,* 9, 1906–1913.

NANNI, L. AND LUMINI, A. 2009b. A supervised method to discriminate between impostors and genuine in biometry. *Expert Syst. Appl. 36,* 7, 10401–10407.

NASEEM, I., TOGNERI, R., AND BENNAMOUN, M. 2008. Sparse representation for ear biometrics. In *Proceedings of the 4th International Symposium on Advances in Visual Computing (ISVC), Part II*. 336–345.

NOSRATI, M., FAEZ, K., AND FARADJI, F. 2007. Using 2D wavelet and principal component analysis for personal identification based on 2D ear structure. In *Proceedings of the IEEE International Conference on Intelligent and Advanced Systems*.

PAN, X., CAO, Y., XU, X., LU, Y., AND ZHAO, Y. 2008. Ear and face based multimodal recognition based on KFDA. In *Proceedings of the IEEE International Conference on Audio, Language and Image Processing (ICALIP)*. 965–969.

PASSALIS, G., KAKADIARIS, I., THEOHARIS, T., TODERICI, G., AND PAPAIOANNOU, T. 2007. Towards fast 3D ear recognition for real-life biometric applications. In *Proceedings of the IEEE Conference on Advanced Video and Signal Based Surveillance*. 39–44.

PHILLIPS, P. J., WECHSLER, H., HUANG, J., AND RAUSS, P. J. 1998. The feret database and evaluation procedure for face recognition algorithms. *Image Vis. Comput. 16,* 5, 295–306.

PHILLIPS, P., MOON, H., RIZVI, S. A., AND RAUSS, P. J. 2000. The feret evaluation methodology for face recognition algorithms. *IEEE Trans. Pattern Anal. Mach. Intell. 22,* 10, 1090–1104.

PRAKASH, S., JAYARAMAN, U., AND GUPTA, P. 2008. Ear localization from side face images using distance transform and template matching. In *Proceedings of the 1st IEEE Workshops on Image Processing Theory, Tools and Applications (IPTA)*.

PRAKASH, S., JAYARAMAN, U., AND GUPTA, P. 2009. A skin-color and template based technique for automatic ear detection. In *Proceedings of the 7th IEEE International Conference on Advances in Pattern Recognition (ICAPR)*.

PUN, K. AND MOON, Y. 2004. Recent advances in ear biometrics. In *Proceedings of the IEEE International Conference on Automatic Face and Gesture Recognition (AFGR)*. 164–169.

PURKAIT, R. AND SINGH, P. 2008. A test of individuality of human external ear pattern: Its application in the field of personal identification. *Forens. Sci. Int. 178,* 112–118.

RAHMAN, M. M. AND ISHIKAWA, S. 2005. Proposing a passive biometric system for robotic vision. In *Proceedings of the 10th International Symposium on Artificial Life and Robotics (AROB)*.

ROSS, A., NANDAKUMAR, K., AND JAIN, A. 2006. *Handbook of Multibiometrics*. Springer.

RUSIGN. 2005. Signature database. University of Rajshahi, Bangladesh.

RUTTY, G., ABBAS, A., AND CROSSLING, D. 2005. Could earprint identification be computerised? An illustrated proof of concept paper. *Int. J. Legal Med. 119,* 333–343.

SAMARIA, F. AND HARTER, A. 1994. Parameterization of a stochastic model for human face identification. In *Proceedings of the 2nd IEEE Workshop on Application of Computer Vision*.

SANA, A. AND GUPTA, P. 2007. Ear biometrics: A new approach. In *Proceedings of the 6th International Conference on Advances in Pattern Recognition*.

SRINIVAS, B. G. AND GUPTA, P. 2009. Feature level fused ear biometric system. In *Proceedings of the 17th IEEE International Conference on Advances in Pattern Recognition*.

THEOHARIS, T., PASSALIS, G., TODERICI, G., AND KAKADIARIS, I. 2008. Unified 3D face and ear recognition using wavelets on geometry images. *Pattern Recogn. 41,* 3, 796–804.

UMIST. 1998. UMIST database. http://www.shef.ac.uk/eee/research/iel/research/face.html.

USTB. 2005. University of science and technology beijing USTB database. http://www1.ustb.edu.cn/resb/en/index.htm

VICTOR, B., BOWYER, K., AND SARKAR, S. 2002. An evaluation of face and ear biometrics. In *Proceedings of the 16th IEEE International Conference on Pattern Recognition (ICPR)*. 429–432.

VIOLA, P. AND JONES, M. 2004. Robust real-time face detection. *Int. J. Comput. Vis. 57,* 2, 137–154.

WANG, Y., MU, Z., AND ZENG, H. 2008. Block-Based and multi-resolution methods for ear recognition using wavelet transform and uniform local binary patterns. In *Proceedings of the 19th IEEE International Conference on Pattern Recognition (ICPR)*. 1–4.

WATABE, D., SAI, H., SAKAI, K., AND NAKAMURA, O. 2008. Ear biometrics using jet space similarity. In *Proceedings of the IEEE Canadian Conference on Electrical and Computer Engineering (CCECE)*.

WOODARD, D., FALTEMIER, T., YAN, P., FLYNN, P., AND BOWYER, K. 2006. A comparison of 3D biometric modalities. In *Proceedings of the IEEE International Conference on Computer Vision and Pattern Recognition (CVPR)*. 57–61.

WRIGHT, J., YANG, A. Y., GANESH, A., SASTRY, S. S., AND MA, Y. 2009. Robust face recognition via sparse representation. *IEEE Trans. Pattern Anal. Mach. Intell. 31,* 2, 210–227.

WU, J., BRUBAKER, S. C., MULLIN, M. D., AND REHG, J. M. 2008. Fast asymmetric learning for cascade face detection. *IEEE Trans. Pattern Analysis Mach. Intell. 30,* 3, 369–382.

XIAOXUN, Z. AND YUNDE, J. 2007. Symmetrical null space lda for face and ear recognition. *Neuro-Comput. 70,* 4-6, 842–848.

XIE, Z. AND MU, Z. 2007. Improved locally linear embedding and its application on multi-pose ear recognition. In *Proceedings of the IEEE International Conference on Wavelet Analysis and Pattern Recognition*.

XIE, Z. AND MU, Z. 2008. Ear recognition using lle and idlle algorithm. In *Proceedings of the 19th IEEE International Conference on Pattern Recognition (ICPR)*. 1–4.

XM2VTSDB. 1999. XM2VTSDB database. http : //www.ee.surrey.ac.uk/CV SSP/xm2vtsdb/

XU, X. AND MU, Z. 2007a. Feature fusion method based on kcca for ear and profile face based multimodal recognition. In *Proceedings of the IEEE International Conference on Automation and Logistics*. 620–623.

XU X. AND MU, Z. 2007b. Multimodal recognition based on fusion of ear and profile face. In *Proceedings of the 4th IEEE International Conference on Image and Graphics (ICIG)*. 598–603.

XU, X., MU, Z., AND YUAN, L. 2007. Feature-Level fusion method based on kfda for multimodal recognition fusing ear and profile face. In *Proceedings of the IEEE International Conference on Wavelet Analysis and Pattern Recognition (ICWAPR)*. Vol. 3. 1306–1310.

YAN, P. AND BOWYER, K. 2005a. Empirical evaluation of advanced ear biometrics. In *Proceedings of the IEEE Conference on Computer Vision and Pattern Recognition (CVPR)*.

YAN, P. AND BOWYER, K. 2005b. Multibiometrics 2D and 3D ear recognition. In *Proceedings of the Audio-and Video-Based Person Authentication Conference (AVBPA)*. 503–512.

YAN, P. AND BOWYER, K. 2006. An automatic 3D ear recognition system. In *Proceedings of the 3rd IEEE International Symposium on 3D Data Processing Visualization and Transmission*. 326–333.

YAN, P. AND BOWYER, K. 2007. Biometric recognition using 3D ear shape. *IEEE Trans. Pattern Anal. Mach. Intell. 29,* 8, 1297–1308.

YAN, P., BOWYER, K., AND CHANG, K. 2005. ICP-Based approaches for 3D ear recognition. In *Proc. SPIE, Biometric Technol. Hum. Identif. II*. 282–291.

YAQUBI, M., FAEZ, K., AND MOTAMED, S. 2008. Ear recognition using features inspired by visual cortex and support vector machine technique. In *Proceedings of the IEEE International Conference on Computer and Communication Engineering*.

YUAN, L. AND MU, Z. 2007. Ear recognition based on 2D images. In *Proceedings of the 1st IEEE International Conference on Biometrics: Theory, Applications, and Systems (BTAS)*.

YUAN, L., MU, Z., AND LIU, Y. 2006a. Multimodal recognition using face profile and ear. In *Proceedings of the IEEE International Symposium on Systems and Control in Aerospace and Astronautics (ISSCAA)*. 887–891.

YUAN, L., MU, Z., ZHANG, Y., AND LIU, K. 2006b. Ear recognition using improved non-negative matrix factorization. In *Proceedings of the 18th IEEE International Conference on Pattern Recognition (ICPR)*. 501–504.

YUAN, L., WANG, Z., AND MU, Z. 2010. Ear recognition under partial occlusion based on neighborhood preserving embedding. *Proc. SPIE, Biometric Technol. Hum. Identif. VII* 7667.

YUAN L. AND ZHANG, F. 2009. Ear detection based on improved adaboost algorithm. In *Proceedings of the 8th IEEE International Conference on Machine Learning and Cybernetics (ICMLC)*.

YUIZONO, T., WANG, Y., S ATOH, K., AND NAKAYAMA, S. 2002. Study on individual recognition for ear images by using genetic local search. In *Proceeding of the IEEE Congress on Evolutionary Computation (CEC)*. 237–242.

ZHANG, H. AND MU, Z. 2008. Ear recognition method based on fusion features of global and local features. In *Proceedings of the IEEE International Conference on Wavelet Analysis and Pattern Recognition*.

ZHANG, H., MU, Z., QU, W., L IU, L., AND ZHANG, C. 2005. A novel approach for ear recognition based on ICA and RBF network. In *Proceedings of the 4th IEEE International Conference on Machine Learning and Cybernetics*. 4511–4515.

ZHANG, Z. AND LIU, H. 2008. Multi-View ear recognition based on b-spline pose manifold construction. In *Proceedings of the 7th IEEE World Congress on Intelligent Control and Automation*.

ZHOU, J., CADAVID, S., AND ABDELMOTTALEB, M. 2010. Histograms of categorized shapes for 3D ear detection. In *Proceedings of the IEEE Conference on Biometrics: Theory, Applications, and Systems (BTAS)*.